Copy 223
RM L55B14

TECH LIBRARY KAFB, NM
0143570

[redacted]

NACA RM L55B14

7606

NACA

RESEARCH MEMORANDUM

AN INVESTIGATION OF THE AERODYNAMIC CHARACTERISTICS OF THIN DELTA WINGS WITH A SYMMETRICAL DOUBLE-WEDGE SECTION AT A MACH NUMBER OF 6.9

By Mitchel H. Bertram and William D. McCauley

Langley Aeronautical Laboratory
Langley Field, Va.

Classification cancelled (or changed to) Uncl
By authority of NASA Tech. Pub.
(OFFICER AUTHORIZED TO CHANGE)
Announcement [illegible] 22 June
By
7 Aug 1961
DATE

[redacted]

NATIONAL ADVISORY COMMITTEE
FOR AERONAUTICS
WASHINGTON
April 14, 1955

[redacted]

K

TECH LIBRARY KAFB, NM
0143570

A

NACA RM L55B14

[redacted]

NATIONAL ADVISORY COMMITTEE FOR AERONAUTICS

RESEARCH MEMORANDUM

AN INVESTIGATION OF THE AERODYNAMIC CHARACTERISTICS OF THIN DELTA WINGS WITH A SYMMETRICAL DOUBLE-WEDGE SECTION AT A MACH NUMBER OF 6.9

By Mitchel H. Bertram and William D. McCauley

SUMMARY

A program to investigate the aerodynamic characteristics of thin delta wings with symmetrical double-wedge sections has been conducted in the Langley 11-inch hypersonic tunnel at a Mach number of 6.9. A family of 5-percent-thick lifting wings with semiapex angles varying from 30° to 8° and one wing which had a $2\frac{1}{2}$-percent thickness and a semiapex angle of 8° were tested over a range of angle of attack from 0° to a maximum of 35°. A series of tests were also made at zero lift for the 5-percent-thick wings and a series of $2\frac{1}{2}$-percent-thick wings with the same semiapex angles. The range of Reynolds numbers for these tests was from 0.7×10^6 to 5.6×10^6 based on root chord.

The lift, drag, and pitching-moment coefficients of the 5-percent-thick wings were adequately predicted by two-dimensional shock-expansion theory when their leading-edge shock waves were attached. When the shock is detached, the lift coefficient obtained at a given angle of attack is considerably less than that given by two-dimensional shock-expansion theory and the efficiency of the wing is lower than that of a two-dimensional wing at lift coefficients greater than that for maximum lift-drag ratio.

The skin-friction coefficients estimated from measurements of the total drag (to a Reynolds number of about 2.8×10^6) appeared to be essentially independent of sweep but higher than the skin-friction coefficients predicted by two-dimensional laminar boundary-layer theory applied to a triangular flat plate. At higher Reynolds numbers on the most highly swept of the wings, transition appeared to occur.

[redacted]

WADC 55-1864K

The centers of pressure obtained experimentally were found to be slightly ahead of the center of area and in good agreement with the centers of pressure given by two-dimensional shock-expansion theory applied to a triangular plan form.

INTRODUCTION

There are relatively few data for lifting wings in the Mach number range above 3. At Mach number 6.9 there are the data obtained by McLellan, Bertram, and Moore (ref. 1), McLellan (ref. 2), and Bertram and McCauley (ref. 3), and at Mach number 4.04 there is the information variously obtained by Ulmann, Lord, Dunning, and Smith (refs. 4 to 7). Reference 8 presents much of the available data for thin delta wings in the range of Mach numbers from 1.6 to 6.9. Much of the data in references 1 to 8 are for plan forms other than delta.

Force predictions for thin delta wings can be obtained through application of the linear theory developed by Puckett, Robinson, Stewart, and Brown (refs. 9 to 13) which allows separate consideration for the effects of thickness (on the drag), camber, and angle of attack. However, the accuracy of these predictions of the aerodynamic forces depends upon whether the shock is attached, since even at the lower supersonic Mach numbers force predictions for wings where shock is detached can be rather poor, and, in addition, at the higher Mach numbers the lift becomes significantly dependent upon the wing section, whereas the lift derived from linear theory is based on a wing with zero thickness. An investigation by Ulmann and Bertram (ref. 8) shows that two-dimensional shock-expansion theory in combination with linear theory may be applied to thin delta wings to obtain accurate predictions of lift-curve slope and minimum drag if a modification of the theory is assumed to account for shock detachment.

This paper reports investigations of two series of thin delta wings which have been conducted in the Langley 11-inch hypersonic tunnel, portions of which have been presented in references 2 and 8. The lifting wings tested in this investigation were 5 percent thick with a symmetrical double-wedge section with semiapex angles varying from 30° to 8° and one wing which was $2\frac{1}{2}$ percent thick with a semiapex angle of 8°. These wings were tested over a range of angle of attack from 0° to a maximum of 35°. A series of tests were also made at zero lift for the 5-percent-thick wings and a series of $2\frac{1}{2}$-percent-thick wings with the same sweep angles. The range of Reynolds number for these tests was from 0.7×10^6 to 5.6×10^6 based on root chord.

SYMBOLS

a	length, in chordwise direction, on wing where boundary-layer transition occurs, in fractions of root chord
b	wing span
c	chord length
Δc	length of sting contained within the wing plan form (see table II)
C_C	chord-force coefficient
C_D	drag coefficient, $\frac{\text{Drag}}{qS}$
C_L	lift coefficient, $\frac{\text{Lift}}{qS}$
$C_{M_{2/3}}$	pitching-moment coefficient about the 2/3 root chord point, $\frac{M_{2/3}}{qSc_r}$
C_N	normal-force coefficient
C_f	average skin-friction coefficient
C.P.	center of pressure measured from wing apex in fractions of root chord
d	sting thickness defined in table II
D	drag
L	lift
M	Mach number
$M_{2/3}$	pitching moment about 2/3 root chord point
m	Mach angle corresponding to free-stream Mach number
R	Reynolds number based on root chord
S	plan-form area

t	thickness
x	dimension of sting defined in table II
y	length of sting outside of wing plan form (see table II)
α	angle of attack of wing
ϵ	semiapex angle of wing
γ	ratio of specific heat at constant pressure to that at constant volume

Subscripts:

i	inviscid
∞	two-dimensional
0	zero angle of attack
r	root

APPARATUS AND METHODS

Tunnel and Nozzles

This investigation was conducted in the Langley 11-inch hypersonic tunnel, an intermittent blowdown tunnel, which, for these tests, utilized a single-step two-dimensional steel nozzle with a central core of uniform flow approximately 5 inches square. The Mach number in this central core is approximately 6.90. A description of the tunnel may be found in reference 14 and a description of the nozzle and its calibration at a stagnation pressure of 25 atmospheres in reference 15.

A two-dimensional nozzle constructed of Invar and designed for a Mach number of 7 was used for a few of the drag tests at zero lift. Invar was used in the construction of this nozzle in order to alleviate the deflection of the first minimum, which occurred in the steel nozzle because of differential heating of the nozzle blocks. In addition, the nozzle was designed so that pressure gradients normal to the horizontal plane of symmetry were a minimum. Preliminary calibrations have indicated a Mach number of 6.86 in the central core of uniform flow which measures about $6\frac{1}{2}$ inches in the vertical direction by about 6 inches horizontally.

Instrumentation

The measurement of the forces on the models was accomplished through the use of two, two-component strain-gage balances of different sensitivities and a balance for the measurement of pitching moment. The more sensitive two-component balance was used in the low angle-of-attack range and measured forces normal and parallel to the wing chord. The other two-component balance measured lift and drag directly and was used for moderate and high angles of attack. The balances are temperature compensated and the sensitivity to uneven heating effects has been reduced to tolerable limits by shielding and insulation. For a more detailed description of the two-component balances, see reference 1.

The base and balance pressures for use with the sting corrections were measured by means of an aneroid-type six-cell recording unit described in reference 14. The stagnation pressure was measured with Bourdon tube gages with an accuracy of 1/2 to 1 percent.

Models and Supports

The wings investigated had symmetrical double-wedge sections in the free-stream direction. The largest wing semiapex angle was 30° and the smallest semiapex angle was 8°. Two sets of wings were tested, one with a thickness ratio of 5 percent, the other with a thickness ratio of $2\frac{1}{2}$ percent. The surfaces were ground and the leading edges were from 0.001 to 0.002 inch thick. The wing designations and dimensions are shown in table I. The mounting stings were essentially the same as those used for the wings reported in reference 3. For one of the wings the sting length on the wing surface was systematically varied. The pertinent dimensions of these stings are shown in table II.

Schlieren System

A schlieren system was used to study flow characteristics and obtain the angle of attack. At present, a single pass system with a Z-shape light path and a horizontal knife edge is employed. Film exposures were of several microseconds duration. The angle of attack was measured from the schlieren film negatives to within 0.2° through the use of an optical comparator.

Surface Film Flow Studies

Surface flow studies of wings 3A, 1C, and 4E were made by photographing the patterns made by streaming graphite and fluorescing mineral oil under ultraviolet light during a run as in reference 3. The wings were coated with SAE 30 lubricating oil before the run and graphite was spotted along the leading edge. The cameras were equipped with suitable filters to photograph the fluorescing oil to best advantage.

TUNNEL CONDITIONS

During the tests, the tunnel was operated at a stagnation temperature of about 1,130° R and through a stagnation pressure range from 15 to 40 atmospheres. For these conditions, the tunnel Reynolds number per inch varied from 0.16×10^6 to 0.41×10^6. An exception to these conditions was the surface film flow tests where the temperature was purposely maintained somewhat lower, averaging about 1,073° R. The air was heated by being passed through an electrical heater with Nichrome tube resistance elements which replaces the storage heater of references 1, 2, 14, and 15. The length of test runs varied from 60 to 75 seconds. The data obtained in the steel nozzle were evaluated at 55 seconds after the start of each run in order to reduce the effects of a slight Mach number variation with time during the run. Nozzle calibrations show that at this time during the run, the Mach number is 6.90 at a stagnation pressure of 33 atmospheres. At stagnation pressures of 21, 25, and 37 atmospheres, calibrations have indicated Mach numbers of 6.84, 6.86, and 6.92, respectively.

PRECISION OF DATA

Errors in coefficients can arise from errors in evaluating the Mach number, stagnation pressure, and angle of attack, as well as inherent errors introduced by aerodynamic heating effects on the balance.

The forces as measured include the force due to the sting support, interference effects of the support, and base- and balance-pressure effects on the support. Corrections due to the lift and drag of the support sting were applied to the coefficients utilizing the forces on similar stings tested without wings. No attempt was made to determine the interference effects between sting and wing. They are believed to be small since the area affected by the shocks from the sting is small and the pressure rise due to sting is believed to be small. The pressures at the base of the sting and in the balance were different when a sting-mounted wing was tested than when a tare sting was tested; therefore a correction was made to the total drag coefficient to account for this pressure difference.

[redacted]

The maximum error possible at several values of C_L and C_D (ΔC_L and ΔC_D) is believed to be shown in the following table:

Balance	C_L	ΔC_L	C_D	ΔC_D
1 (sensitive)	0.01	0.0025	0.006	0.0004 - 0.0007
	.04	.0032	.04	.0026 - .0032
	.13	.0065		
2	.22	.010	.07	.0042 - .0084
	.45	.016	.35	.016

Wing 4E was tested through a range of Reynolds numbers at zero angle of attack; the maximum error possible at different Reynolds numbers is believed to be as follows:

R	$\frac{\Delta C_D}{C_D}$
2.4×10^6	0.14
3.0	.11
4.0	.09
5.0	.07

In the evaluation of moment coefficients and consequently, center of pressure, there is an additional source of error introduced by the transference of the moment as measured about the balance center of moment to the desired point on the wing. The maximum error in individual moment data points (ΔC_M and ΔC.P.) is believed to be as follows:

Wing	ΔC_M
1A	0.0012
2A	.0010
3A	.0007
4A	.0006
4D	.0006

α, deg	ΔC.P.
2	0.04
4	.02
8	.01

[redacted]

RESULTS AND DISCUSSION

Lift and Drag Characteristics

Figure 1 presents the lift and drag coefficients and the lift-drag ratio as a function of angle of attack for the wings tested. The solid lines are the values of these parameters predicted for the airfoil section (in the streamwise direction) by the two-dimensional shock-expansion theory, whereas the dashed lines are the wing coefficients obtained from the Newtonian impact theory. The values of the coefficients obtained from shock-expansion theory for a flat plate and for diamond sections with $2\frac{1}{2}$- and 5-percent-thickness ratios are given in table III. The aerodynamic coefficients obtained from Newtonian impact theory were calculated as shown in appendix A of reference 3. The same values of skin-friction coefficient have been added to the pressure-drag coefficients from both the shock-expansion and impact theories, the skin-friction coefficients being estimated as given in a later section concerning the drag at zero angle of attack.

Lift coefficient as a function of angle of attack.- The lift coefficients of the 5-percent-thick wing having a semiapex angle of 30° (fig. 1(a)) are close to, though slightly higher than, the predictions of two-dimensional shock-expansion theory up to the angle of attack for shock detachment, $\alpha = 17.8^\circ$ (angles of attack for shock detachment computed according to appendix B of ref. 3), and considerably higher than the values given by impact theory. As the angle of attack is increased above the angle for shock detachment, the experimental values of the lift coefficient drop markedly below the predictions of shock-expansion theory though not nearly as low as the values given by impact theory.

As the semiapex angle of these wings is decreased (figs. 1(b) to 1(d)), the loss in C_L increases at angles of attack greater than that for shock detachment. The values for the coefficients given by the Newtonian impact theory, in general, underestimate the values obtained experimentally, except at the higher angles of attack where the experimental values approach those given by impact theory and in some cases fall on the curve given by impact theory. From the experience of Penland (ref. 16), who tested cylinders up to very high angles of attack, it may be inferred that such agreement occurs only at a crossover point for the experimental and impact theory curves and at still higher angles of attack the impact theory can be expected to overestimate the lift.

Figures 1(d) and 1(e) may be compared to show the effect of thickness ratio where the shock is detached at all angles of attack. The experimental data show that the $2\frac{1}{2}$-percent-thick wing with $\epsilon = 8^\circ$

(wings 4D and 4E) has a higher lift than the 5-percent-thick wing with $\epsilon = 8^\circ$ (wing 4A) over the entire range of angle of attack, 0° to about 35°. If the wings were two-dimensional, shock-expansion theory indicates that the lift of the $2\frac{1}{2}$-percent-thick wing would be less than that of the 5-percent-thick wing up to an angle of attack between 20° and 25° and the reverse would be true above this angle of attack. The more severe effect of shock detachment on the 5-percent-thick wing apparently has a large enough effect to cause the lift for this wing to be lower than that for the $2\frac{1}{2}$-percent-thick wing at all angles of attack.

In order to show more readily the change in experimental C_L for the various semiapex angles in comparison to the values of C_L predicted by the two-dimensional shock-expansion theory, as a function of angle of attack, figures 2 and 3 have been prepared. Figure 2 presents results for the 5-percent-thick wings with semiapex angles of 30°, 20°, and 13° and figure 3 presents results for wings with semiapex angles of 8° and thickness ratios of 0.050 and 0.025.

From figure 2, the lift of the wing with $\epsilon = 30^\circ$ can be seen to average about 3 percent higher than that for a two-dimensional wing up to the angle of attack for shock detachment. The rapid loss in lift immediately after shock detachment is readily apparent. The increase in lift over the two-dimensional value before shock detachment does not appear to be present for the wing with $\epsilon = 20^\circ$. All three wings shown in figure 2 exhibit the characteristic drop in lift above the angle of attack for shock detachment.

Figure 3 shows the more severe effects of shock detachment on the 5-percent-thick wing with $\epsilon = 8^\circ$ as compared to the $2\frac{1}{2}$-percent-thick wing. The greater loss in lift for the 5-percent-thick wing can be clearly seen. This same effect on initial lift-curve slope over a considerable Mach number range has been shown in reference 8.

At the higher angles of attack where all the wings investigated had detached leading-edge shocks, say about $\alpha = 26^\circ$, a comparison of figure 3 of reference 3 with figures 2 and 3 given here shows that the loss of lift both percentagewise and in the absolute sense for the relatively thick wings of reference 3 is considerably greater than for the wings of this investigation when compared with their corresponding two-dimensional wings.

Drag coefficient as a function of angle of attack.- For the drag coefficient at angle of attack, much the same comments apply as for the lift coefficients considered previously, but because of the shape of the drag curve, the effects are not so apparent as for the lift. When the leading-edge shock is attached, the drag coefficient is close to the prediction given by shock-expansion theory (figs. 1(a) and 1(b)). When the angle of attack is increased beyond the angle of shock detachment, the experimental values of C_D drop below the theory (figs. 1(a) to 1(c)). As the semiapex is decreased when the shock is detached the drag coefficient at a given angle of attack is decreased still further below the value given by shock-expansion theory (figs. 1(a) to 1(d)).

Drag coefficient at zero angle of attack.- Figure 4 has been prepared to show the effect of Reynolds number on the minimum drag of both the 5-percent-thick and the $2\frac{1}{2}$-percent-thick series of wings. Results from wing 4E have not been included in this figure. The theoretical values of the two-dimensional wave drag given by shock-expansion theory and the total drag obtained by adding this wave drag to estimated values of laminar skin friction have also been included.

For the essentially two-dimensional wings of references 1 and 17, the theoretical skin-friction coefficients for a flat plate in conjunction with the inviscid pressure drag were found to be in good agreement with the experimental results. In order to make a similar comparison for triangular wings, the theoretical constant for an insulated flat plate (as given in ref. 18) was modified by using an effective chord which for a triangular flat plate is 9/16 of the root chord assuming no deviation of the streamlines from the free stream direction. The resulting skin-friction relationship for a triangular flat plate for the conditions of the present tests is $C_f\sqrt{R} = 3.25$. If conical flow is assumed $C_f\sqrt{R} = 2.81$. These theoretical values for the boundary layer constants are expected to indicate only the lowest values of skin-friction coefficients. In this particular case, the theoretical predictions of skin friction at zero lift based on the above coefficients underestimate the skin-friction derived from the experimental results. One reason for the poor agreement between experiment and theory is perhaps the self-induced (negative) pressure gradient (ref. 18) which is not considered in the theory. This self-induced pressure gradient increases the wing pressure drag over the case without pressure gradient and, also, would be expected to increase the value of C_f.

The laminar skin-friction values used in figures 1 and 4 were empirically determined from an examination of the data for the wings with attached shocks from both this investigation and that of reference 3. For both the 5-percent-thick wings of this investigation and the wings of reference 3 which were 8 percent thick, good agreement with the data from the wings with attached shocks was obtained when $C_f\sqrt{R} = 4.89$ and the pressure-drag coefficient was assumed to be equal to that for the wing section (in the streamwise direction).

In figure 4 it can be seen that the agreement between the estimated and experimental results is essentially independent of sweep angle although it is better in general for the B series of wings than for the A series of wings. In general, the B series wings had relatively smaller stings than the A series wing (see table II) and many of the discrepancies between similar wings shown in figure 4 may be due to differences in sting effects.

Because of the effect of shock detachment and the consequent conical nature of the flow field, the drag of the $\epsilon = 8^{\circ}$ wings might be expected to be slightly below the values given by shock-expansion theory (ref. 8); however, such a decrease in the pressure drag could not explain the large decreases shown in figure 4(d). Another possibility is, of course, an incorrect assumption for the laminar skin friction.

In order to obtain more accurate data over a wider Reynolds number range and to investigate sting effects more fully, a large $2\frac{1}{2}$-percent-thick wing with $\epsilon = 8^{\circ}$ was constructed on which the sting length on the wing surface was systematically varied (see table II, wings 4E-1, 4E-2, and 4E-3). The results of the tests on this wing are shown in figure 5. Included in this figure are tests which were made in a recently installed nozzle whose contour plates were machined from Invar. The design of this nozzle is different in several respects from that of the steel nozzle used for the bulk of the tests (see preceding section entitled "Apparatus and Methods").

Two effects of the sting were anticipated. The shock from the sting might increase pressures on the rear surface of the wing near the sting, which would decrease the drag, and the shock might also cause boundary-layer transition, which would increase the drag. It might be mentioned that if the shock from the sting fixes transition on the wing, calculations (utilizing ref. 17) have indicated that this would be difficult to determine from the trend of drag coefficient with Reynolds number since such an effect would manifest itself as an apparent change in the constant determining the laminar skin-friction coefficient, so long as the line along which transition occurs does not approach the leading edge too closely.

From overall consideration of these datum points and their accuracies, there does not appear to be any appreciable difference between the results from wing 4E in the different nozzles or for the various sting lengths tested. However, it is apparent that at about a Reynolds number of 3×10^{6} where the data become more accurate there is a difference between the trend of the theoretical drag curves that would be expected with a laminar boundary layer and the trend which was obtained experimentally.

Calculations were made to determine if boundary-layer transition would explain the experimental trend. Drag coefficients were computed by assuming that transition occurred along lines parallel to the leading edges on a triangular flat plate. This assumption is based on results at Mach number of 2.01 and 2.50 in reference 19 and unpublished data obtained in the Langley 9- by 9-inch Mach number 4 blowdown jet. The calculations were made assuming various Reynolds numbers for transition and indicated that boundary-layer transition is a possible cause of the difference in the trend between the experimental data and that which is predicted for a laminar boundary layer.

The lift-drag ratios of the wings having the same area (the A and D series wings) are compared in figures 6 and 7. Figure 6 shows the effect of decreasing the semiapex angle of 5-percent-thick wings from 30° to 8° and figure 7 shows the effect of changing the thickness ratio of the wing with the 8° semiapex angle.

Up to the optimum lift coefficient the L/D of the wing shows a slight trend toward increasing lift-drag ratio with decreasing semiapex angle, which in this case can be attributed to an increase in the effective Reynolds number with decreasing ϵ. This same trend was strongly exhibited by the wings of reference 3 which had 8-percent-thick airfoil sections with the maximum thickness at the 18-percent-chord point, though in that case more than a Reynolds number effect was apparently involved. Above the optimum lift coefficient, the trend is for the L/D ratios to decrease with decreasing ϵ when the shock is detached, which is also the trend shown in reference 3.

Comparison of the theoretical and experimental effects of decreasing the wing semiapex angle (decreasing the aspect ratio) and the wing thickness ratio is shown in figures 6 and 7. These theoretical curves are based on a modification to shock-expansion theory according to the percentage changes in C_L and C_D due to sweep predicted by Newtonian theory for double-wedge section delta wings as presented in appendix A of reference 3. Actually, the calculations show that for thin wings such as these the Newtonian theory predicts only small three-dimensional effects insofar as the efficiency of the wing is concerned. The experimental results show much larger effects of sweep than are indicated by the theory, though the variation of L/D with C_L is predicted rather well by the shock-expansion theory for the wings with $\epsilon = 30^{\circ}$ and $\epsilon = 20^{\circ}$.

Figure 7 illustrates the effect of thickness ratio where the shock is detached at all angles of attack. The $2\frac{1}{2}$-percent-thick wing is found to be more efficient throughout the range of lift coefficients shown. Though the agreement of both wings with their corresponding theoretical curve is considered poor, the theoretical curves do indicate correctly the magnitude of the difference between the two wings. Also included in figure 7 is the unmodified two-dimensional shock-expansion theory with $C_f = 0.0032$ included in the drag. The amount of three-dimensional effect given by Newtonian impact theory can be clearly seen.

When the results shown in figures 6 and 7 are compared to the experimental results presented in reference 3, all of these wings are found to be more efficient than the most efficient wing shown in that report.

Center of Pressure and Moment Coefficient

As shown in figure 8, moment data indicate the center of pressure to be slightly ahead of the center of area as was the case for the delta wings reported in reference 3 at this Mach number. Changes in apex angle in general do not appear to have a noticeable effect on the center-of-pressure location. At very low angles of attack, there does appear to be an effect of apex angle. However, there is doubt as to whether this effect shown by the low angle-of-attack data actually exists because of not only the considerations of data accuracy presented previously in this paper, but also to considerations of the correction due to the moment contributed by the sting to the original data. The assumption for the sting center of pressure, since the stings were not tested on the moment balance, becomes somewhat in doubt at very low angles of attack.

The center-of-pressure data are in remarkably good agreement with the centers of pressure given by two-dimensional shock-expansion theory (table III) applied to a triangular plan form where

$$C.P. = \frac{2}{3}\left[(C.P.)_{\infty} + \frac{1}{2}\right]$$

The theoretical moment-coefficient curves shown at the top of figure 8 were obtained by using this center of pressure together with the two-dimensional C_N. Where the shock is attached to the wing, the agreement with the theoretical curve is good; where the shock is detached, the experimental moment coefficients lie below the theoretical curve due mainly to the decrease in normal-force coefficient. The smaller the apex angle in the shock-detached region, the smaller the moment coefficient for a given angle of attack. For a given lift coefficient, all the wings have practically the same moment coefficient.

Schlieren Photographs

Figures 9 to 13 present schlieren photographs taken during the course of this investigation. For all the wings, the shock patterns shown in the side views are similar. The top view schlieren photographs show that theory and experiment in general agree as to the leading-edge shock attachment and detachment as a function of both sweep angle and angle of attack.

Surface Film Flow Studies

Oil flow studies on the surface of wings 1C, 3A, 4E-2, and 4E-3 (figs. 14 and 15) were made to show the flow in the boundary layer next to the surface. The tracings of graphite particles in fluorescing oil during a run were observed. The outlines of the wings have been sketched in the flow photographs for reference purposes.

The results on the lower surface of wing 3A (fig. 14) are essentially the same at zero lift and angles of attack. On the front surfaces, the flow is essentially parallel to, but flowing in slightly, toward the root chord. As the flow goes over the ridge line to the rear surface, the increase in the normal component of velocity causes an increased flow toward the root chord. However, the surface flow quickly straightens after the ridge line and continues essentially parallel to the stream flow. As was the case for the delta wings of reference 3, there is an indication of a disturbance starting just behind the thickness peak and extending out as a ray on either side of the center line.

On the upper surface of wing 3A (fig. 14) at angle of attack, the flow phenomena appear to be more complicated. On the front surfaces, the flow turns out slightly from the root chord and there is a high shear region at the root chord forward of the maximum thickness. As the flow expands over the ridge line to the rear surface, it turns in toward the root chord after which it separates. A shock is probably present where the separation occurs. The surface flow patterns are similar to those obtained for the delta wings reported in reference 3. The sting appears to interfere somewhat with the surface flow phenomena. Schlieren photographs corresponding to those of the surface flow studies for this wing are shown in figure 11.

Figure 15(a) shows the flow soon after starting on wing 1C and the interference region due to the sting is somewhat masked; however, the oil can be seen to be flowing slightly toward the root chord on the visible part of the front surfaces, and turning still more toward the root chord over the ridge line. From a consideration of the nonviscous flow at zero lift on the front surfaces, the flow should turn slightly away from the root chord because of the decrease of the normal velocity component through the shockwave; however, the effect of the pressure gradient in the central conical flow field and the effects of boundary-layer-displacement thickness on the pressures would tend to turn the air in the viscous layer slightly toward the root chord. In addition, in the region of the central ridge line and on the rear surface the two-dimensional velocity normal to the ridge line is increased causing the resultant flow to turn more toward the root chord. It should be recognized, however, that the oil flow at the surface which is within the boundary layer should not be arbitrarily taken as indicating the flow directions outside the boundary layer. This is shown by the work of Hatch and Hargrave (ref. 20) and Hatch and Gallagher (ref. 21), where by the use of wind vanes of different elevations above the surface, they were able to show the change in flow angle with vertical displacement.

Two views have been presented of wing 4E (figs. 15(b) and 15(c)) to study the effects of the sting on the flow over the wing. This figure indicates that decreasing the support length on the wing by 25 percent decreased the interference area by about 57 percent. On the front surfaces, the flow is essentially parallel to the root chord. As the flow goes over the ridge line, it is turned toward the root chord by the expansion of the normal-flow component and, where it is influenced by the sting disturbance, the oil apparently tends to flow out along the disturbance boundary.

CONCLUSIONS

A program to investigate the aerodynamic characteristics of thin delta wings with a symmetrical double-wedge section has been conducted in the Langley 11-inch hypersonic tunnel at a Mach number of 6.9. A family of 5-percent-thick lifting wings with semiapex angles varying from 30° to 8° and one wing which had a $2\frac{1}{2}$ -percent thickness and semiapex angle of 8° were tested over a range of angle of attack from 0° to a maximum of 35°. A series of tests were also made at zero lift for the 5-percent-thick wings and a series of $2\frac{1}{2}$ -percent-thick wings with the same semiapex angles. The range of Reynolds number for these tests was from 0.7×10^6 to 5.6×10^6 based on root chord. An analysis of the results of this investigation has led to the following observations:

1. Two-dimensional shock-expansion theory adequately predicts the lift, drag, and moment coefficients for these delta wings when the leading-edge shock is attached.

2. When the shock is detached, the lift coefficient obtained at a given angle of attack is considerably reduced from that given by

two-dimensional theory and the efficiency of the wing is lower than that of a two-dimensional wing beyond the lift coefficient at which maximum lift-drag ratio occurs.

3. The skin-friction coefficients estimated from measurements of the total drag (to a Reynolds number of about 2.8×10^6) appeared to be essentially independent of sweep but higher than the skin-friction coefficients predicted by two-dimensional laminar boundary-layer theory applied to a triangular flat plate. At higher Reynolds numbers, transition of the boundary layer appeared to occur.

4. The centers of pressure obtained experimentally were found to be slightly ahead of the center of area and in good agreement with the centers of pressure given by two-dimensional shock-expansion theory applied to a triangular plan form.

Langley Aeronautical Laboratory,
National Advisory Committee for Aeronautics,
Langley Field, Va., February 1, 1955.

REFERENCES

1. McLellan, Charles H., Bertram, Mitchel H., and Moore, John A.: An Investigation of Four Wings of Square Plan Form at a Mach Number of 6.86 in the Langley 11-Inch Hypersonic Tunnel. NACA RM L51D17, 1951.

2. McLellan, Charles H.: Exploratory Wind-Tunnel Investigation of Wings and Bodies at $M = 6.9$. Jour. Aero. Sci., vol. 18, no. 10, Oct. 1951, pp. 641-648.

3. Bertram, Mitchel H., and McCauley, William D.: Investigation of the Aerodynamic Characteristics at High Supersonic Mach Numbers of a Family of Delta Wings Having Double-Wedge Sections With the Maximum Thickness at 0.18 Chord. NACA RM L54G28, 1954.

4. Ulmann, Edward F., and Lord, Douglas R.: An Investigation of Flow Characteristics at Mach Number 4.04 Over 6- and 9-Percent-Thick Symmetrical Circular-Arc Airfoils Having 30-Percent-Chord Trailing-Edge Flaps. NACA RM L51D30, 1951.

5. Ulmann, Edward F., and Dunning, Robert W.: Aerodynamic Characteristics of Two Delta Wings at Mach Number 4.04 and Correlations of Lift and Minimum-Drag Data for Delta Wings at Mach Numbers From 1.62 to 6.9. NACA RM L52K19, 1952.

6. Dunning, Robert W., and Ulmann, Edward F.: Aerodynamic Characteristics at Mach Number 4.04 of a Rectangular Wing of Aspect Ratio 1.33 Having a 6-Percent-Thick Circular-Arc Profile and a 30-Percent-Chord Full-Span Trailing-Edge Flap. NACA RM L53D03, 1953.

7. Dunning, Robert W., and Smith, Fred M.: Aerodynamic Characteristics of Two Delta Wings and Two Trapezoidal Wings at Mach Number 4.04. NACA RM L53D30a, 1953.

8. Ulmann, Edward F., and Bertram, Mitchel H.: Aerodynamic Characteristics of Low-Aspect-Ratio Wings at High Supersonic Mach Numbers. NACA RM L53I23, 1953.

9. Puckett, Allen E.: Supersonic Wave Drag of Thin Airfoils. Jour. Aero. Sci., vol. 13, no. 9, Sept. 1946, pp. 475-484.

10. Robinson, A.: Lift and Drag of a Flat Delta Wing at Supersonic Speeds. Tech. Note No. Aero.1791, British R.A.E., June 1946.

[redacted]

11. Stewart, H. J.: The Lift of a Delta Wing at Supersonic Speeds. Quarterly Appl. Math., vol. IV, no. 3, Oct. 1946, pp. 246-254.

12. Brown, Clinton E.: Theoretical Lift and Drag of Thin Triangular Wings at Supersonic Speeds. NACA Rep. 839, 1946. (Supersedes NACA TN 1183.)

13. Puckett, A. E., and Stewart, H. J.: Aerodynamic Performance of Delta Wings at Supersonic Speeds. Jour. Aero. Sci., vol. 14, no. 10, Oct. 1947, pp. 567-578.

14. McLellan, Charles H., Williams, Thomas W., and Bertram, Mitchel H.: Investigation of a Two-Step Nozzle in the Langley 11-Inch Hypersonic Tunnel. NACA TN 2171, 1950.

15. McLellan, Charles H., Williams, Thomas W., and Beckwith, Ivan E.: Investigation of the Flow Through a Single-Stage Two-Dimensional Nozzle in the Langley 11-Inch Hypersonic Tunnel. NACA TN 2223, 1950.

16. Penland, Jim A.: Aerodynamic Characteristics of a Circular Cylinder at Mach Number 6.86 and Angles of Attack Up to 90°. NACA RM L54A14, 1954.

17. Van Driest, E. R.: Turbulent Boundary Layer in Compressible Fluids. Jour. Aero. Sci., vol. 18, no. 3, March 1951, pp. 145-160, 216.

18. Bertram, Mitchel H.: An Approximate Method for Determining the Displacement Effects and Viscous Drag of Laminar Boundary Layers in Two-Dimensional Hypersonic Flow. NACA TN 2773, 1952.

19. Lukasiewicz, J., Stewart, J. D., and LaBerge, J. G.: Half-Model Tests of Two Small Aspect Ratio Delta Wings at Subsonic, Transonic and Supersonic Speeds. Lab. Rep. LR-92, Nat. Aero. Establishment, (Ottawa), Jan. 1954.

20. Hatch, John E., Jr., and Hargrave, L. Keith: Effects of Reynolds Number on the Aerodynamic Characteristics of a Delta Wing at Mach Number of 2.41. NACA RM L51H06, 1951.

21. Hatch, John E., Jr., and Gallagher, James J.: Aerodynamic Characteristics of a 68.4° Delta Wing at Mach Numbers of 1.6 and 1.9 Over a Wide Reynolds Number Range. NACA RM L53I08, 1953.

TABLE I

WING DIMENSIONS

Wing designation	Semiapex angle, deg	Sketch	Chord, in.	Span, in.	Area, sq in.	Location of maximum thickness, percent c	Thickness ratio	Aspect ratio
1A	30	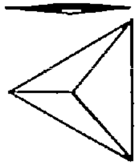	3.464	4.000	6.93	0.50	0.050	2.309
1B	30		4.363	5.038	10.99	.50	.050	2.309
1C	30		4.363	5.038	10.99	.50	.025	2.309
2A	20	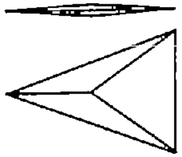	4.363	3.176	6.93	0.50	0.050	1.456
2B	20		5.495	4.000	10.99	.50	.050	1.456
2C	20		5.495	4.000	10.99	.50	.025	1.456
3A	13	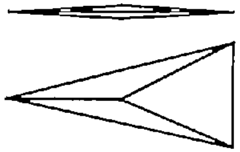	5.478	2.529	6.93	0.50	0.050	0.924
3B	13		6.900	3.186	10.99	.50	.050	.924
3C	13		6.900	3.186	10.99	.50	.025	.924
4A	8	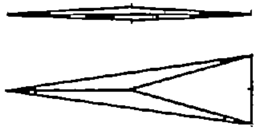	7.021	1.974	6.93	0.50	0.050	0.562
4D	8		7.021	1.974	6.93	.50	.025	.562
4E	8		14.042	3.947	27.71	.50	.025	.562

TABLE II

STING DIMENSIONS IN RELATION TO WING

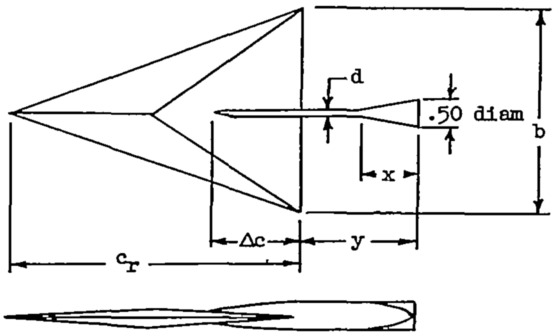

Wing	$\Delta c/c_r$	y/c_r	$\frac{d}{b}$	$\frac{x}{y}$
1A	0.37	0.70	0.037	0.40
1B	.38	.54	.031	.52
1C	.39	.54	.018	.52
2A	.32	0.55	0.049	0.48
2B	.26	.44	.023	.52
2C	.32	.43	.023	.53
3A	.30	0.44	0.062	0.52
3B	.21	.34	.029	.53
3C	.25	.35	.029	.52
4A	.27	0.34	0.079	0.45
4D	.27	.35	.074	.56
4E-1	.43	.13	.055	1.00
4E-2	.28	.13	.055	1.00
4E-3	.19	.13	.055	1.00

[redacted]

TABLE III

THE COEFFICIENTS OBTAINED FROM SHOCK-EXPANSION THEORY FOR A SYMMETRICAL DOUBLE-WEDGE SECTION AIRFOIL, $M = 6.90$

α, deg	c_N	c_C	c_L	c_D	L/D	C.P.
Flat plate $\left(\frac{t}{c} = 0\right)$						
0	0	0	0	0	∞	-----
1	.01025	0	.01025	.00018	57.29	0.500
2.5	.02590	0	.0259	.0011	22.90	.500
5	.05400	0	.0538	.0047	11.43	.500
7.5	.08632	0	.0856	.0113	7.60	.500
10	.1249	0	.1230	.0217	5.67	.500
12.5	.1702	0	.1662	.0368	4.51	.500
15	.2224	0	.2148	.0576	3.73	.500
20	.3487	0	.3277	.1193	2.75	.500
25	.5005	0	.4536	.2115	2.14	.500
30	.6829	0	.5914	.3414	1.73	.500
35	.8892	0	.7284	.5100	1.43	.500
$\frac{t}{c} = 0.025$						
0	0	0.00037	0	.00037	0	-----
1	.01040	.00037	.01039	.00055	18.84	0.448
1.43	.01489	.00037	.01488	.00074	20.07	.448
2.5	.02628	.00039	.02624	.00154	17.08	.449
5	.05480	.00043	.05455	.00520	10.48	.450
7.5	.08726	.00051	.08645	.01190	7.26	.454
10	.1255	.00062	.1235	.02240	5.51	.456
12.5	.1695	.00073	.1653	.03740	4.42	.459
15	.2207	.00085	.2129	.05794	3.68	.462
20	.3421	.00113	.3210	.1180	2.72	.467
25	.4960	.00134	.4490	.2108	2.13	.473
30	.6760	.00155	.5847	.3394	1.72	.477
35	.8858	.00172	.7246	.5094	1.42	.481
$\frac{t}{c} = 0.050$						
0	0	0.00149	0	0.00149	0	-----
1	.01089	.00150	.01086	.001690	6.43	0.404
2.5	.02742	.00155	.02733	.002745	9.96	.404
2.86	.03146	.00158	.03134	.003148	9.96	.405
5	.05662	.00175	.05625	.006674	8.43	.407
7.5	.08988	.00204	.08884	.01376	6.46	.412
10	.1283	.00242	.1259	.02466	5.11	.417
12.5	.1730	.00282	.1683	.04020	4.19	.422
15	.2234	.00328	.2149	.06099	3.52	.427
20	.3461	.00426	.3237	.1224	2.65	.438
25	.4970	.00517	.4483	.2147	2.09	.448
30	.6777	.00598	.5839	.3440	1.70	.456
35	.8870	.00668	.7228	.5143	1.40	.462

[redacted]

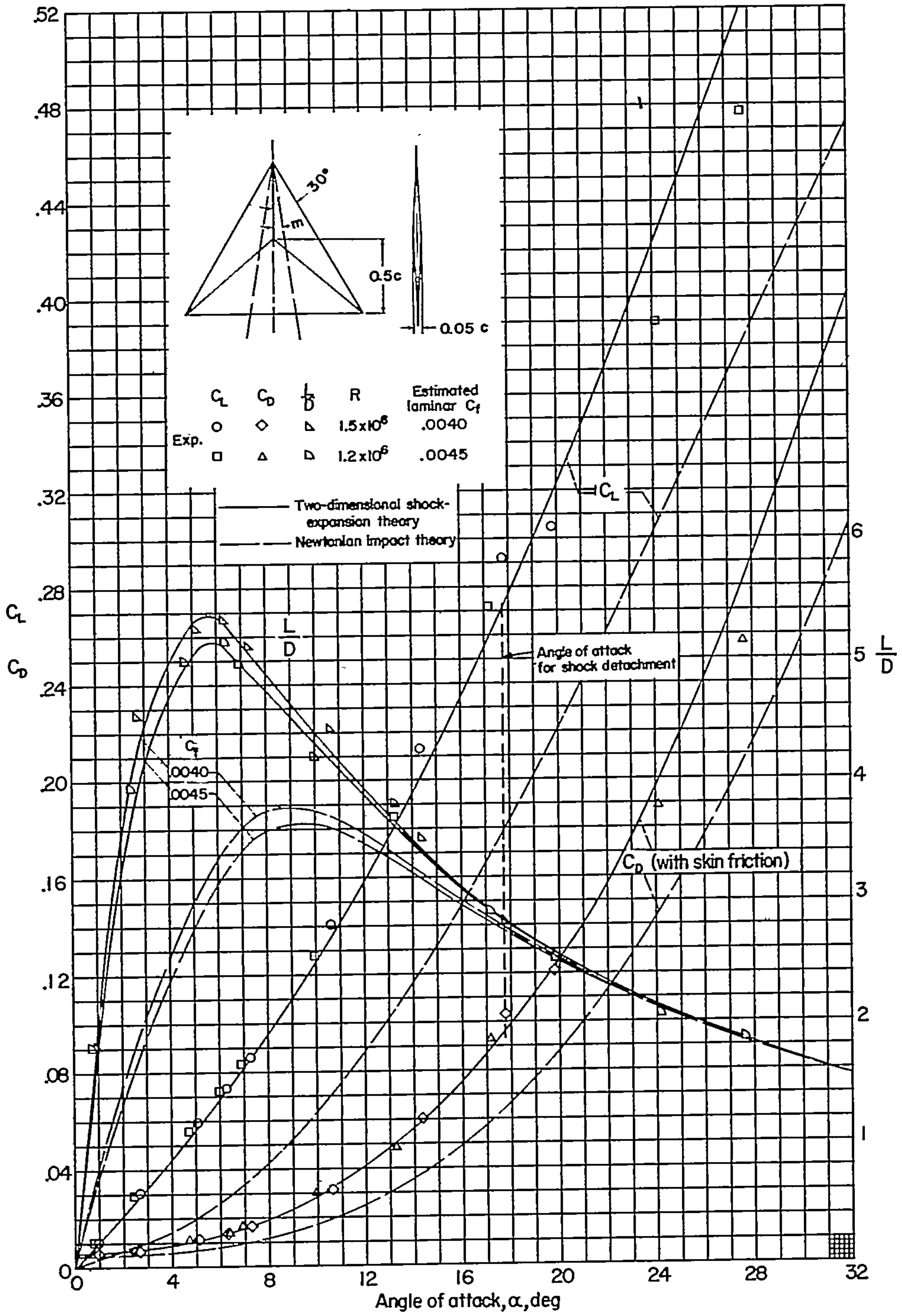

(a) $\epsilon = 30^\circ$ (wings 1A and 1B).

Figure 1.- The lift and drag coefficients and lift-drag ratios of a series of delta wings with the maximum thickness at 50 percent chord as a function of angle of attack. M = 6.9.

[redacted]

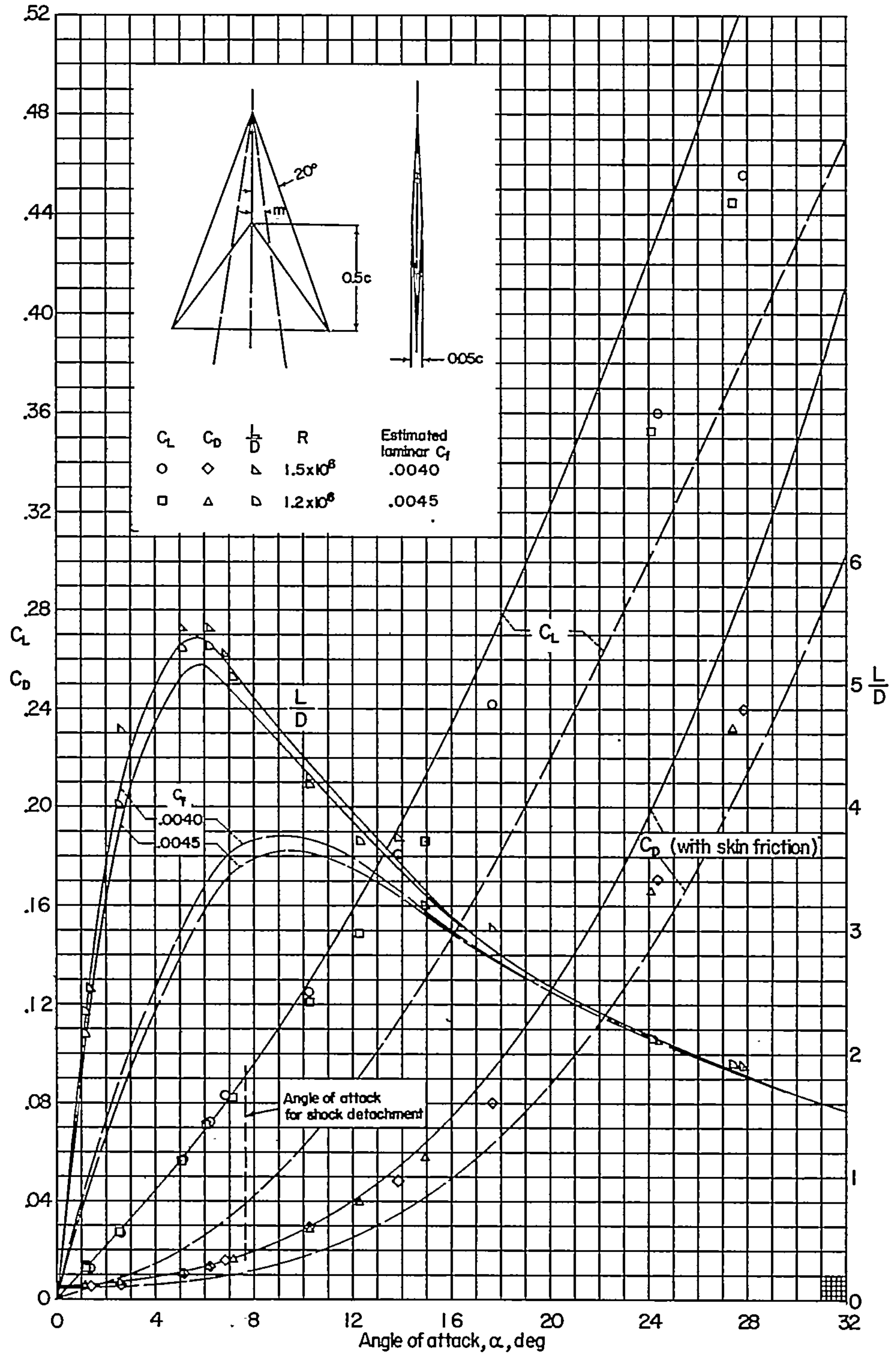

(b) $\epsilon = 20^\circ$ (wing 2A).

Figure 1.- Continued.

[redacted]

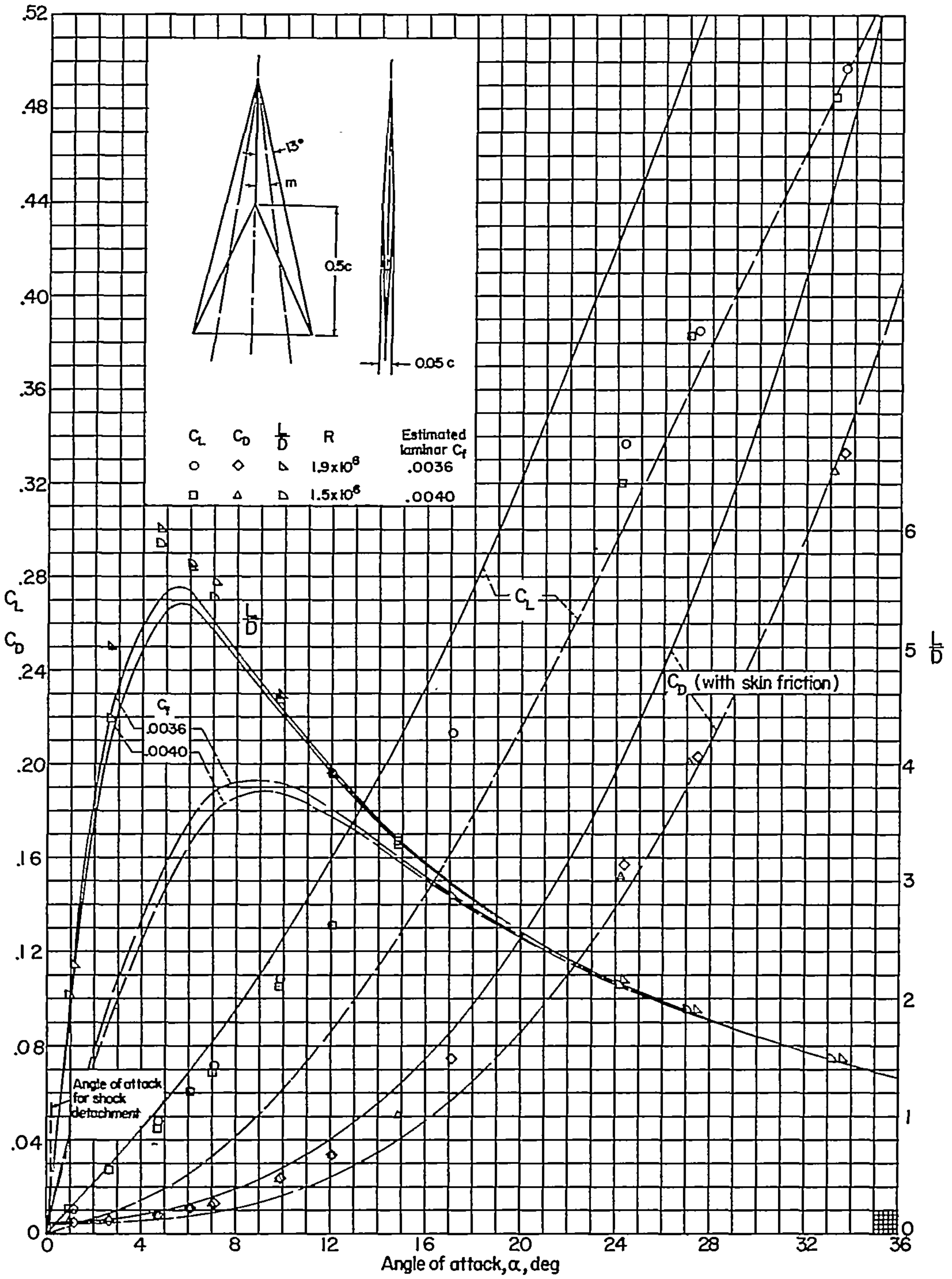

(c) $\epsilon = 13^{\circ}$ (wing 3A).

Figure 1.- Continued.

[redacted]

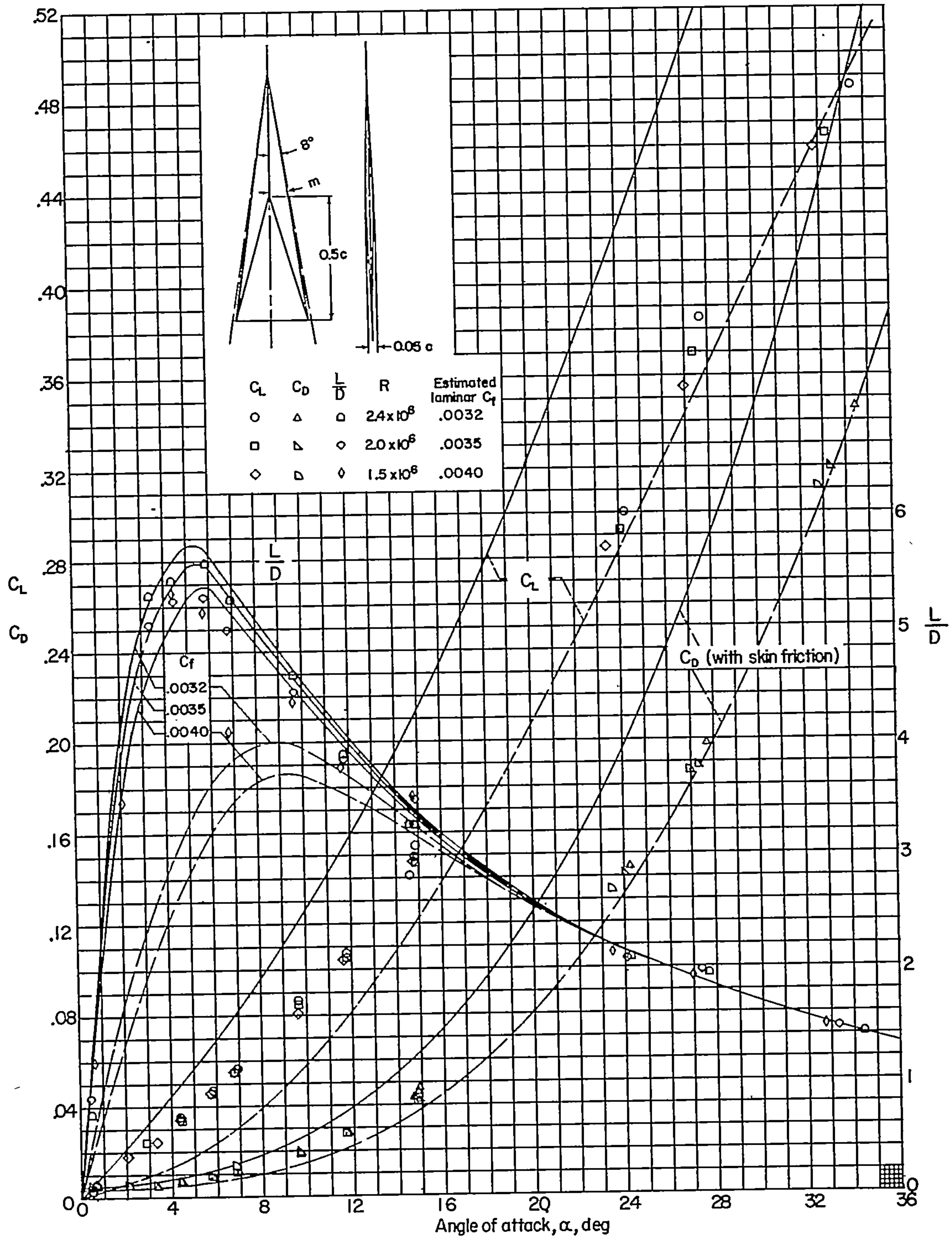

(d) ε = 8° (wing 4A).

Figure 1.- Continued.

[redacted]

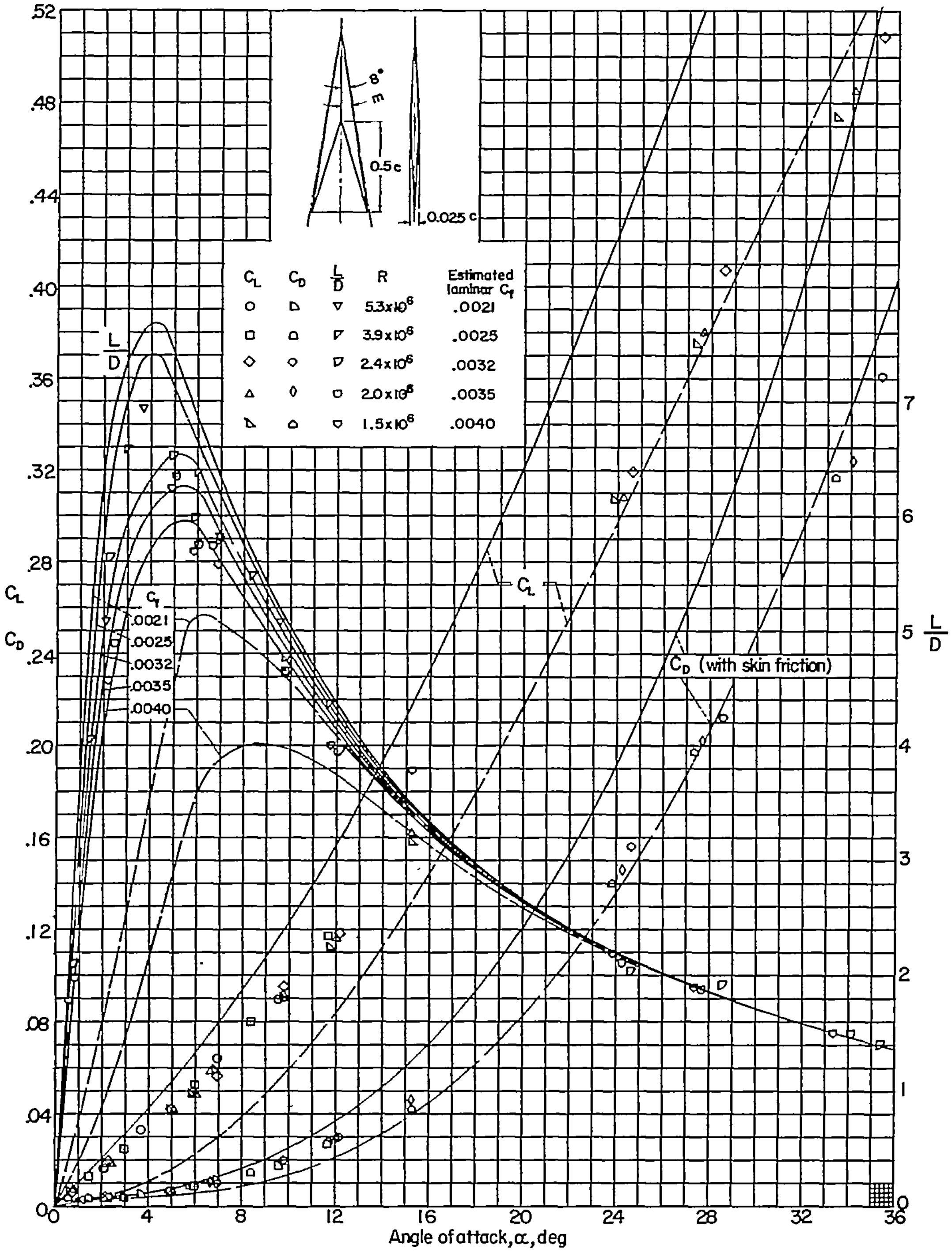

(e) $\epsilon = 8^{\circ}$ (wings 4D and 4E).

Figure 1.- Concluded.

[redacted]

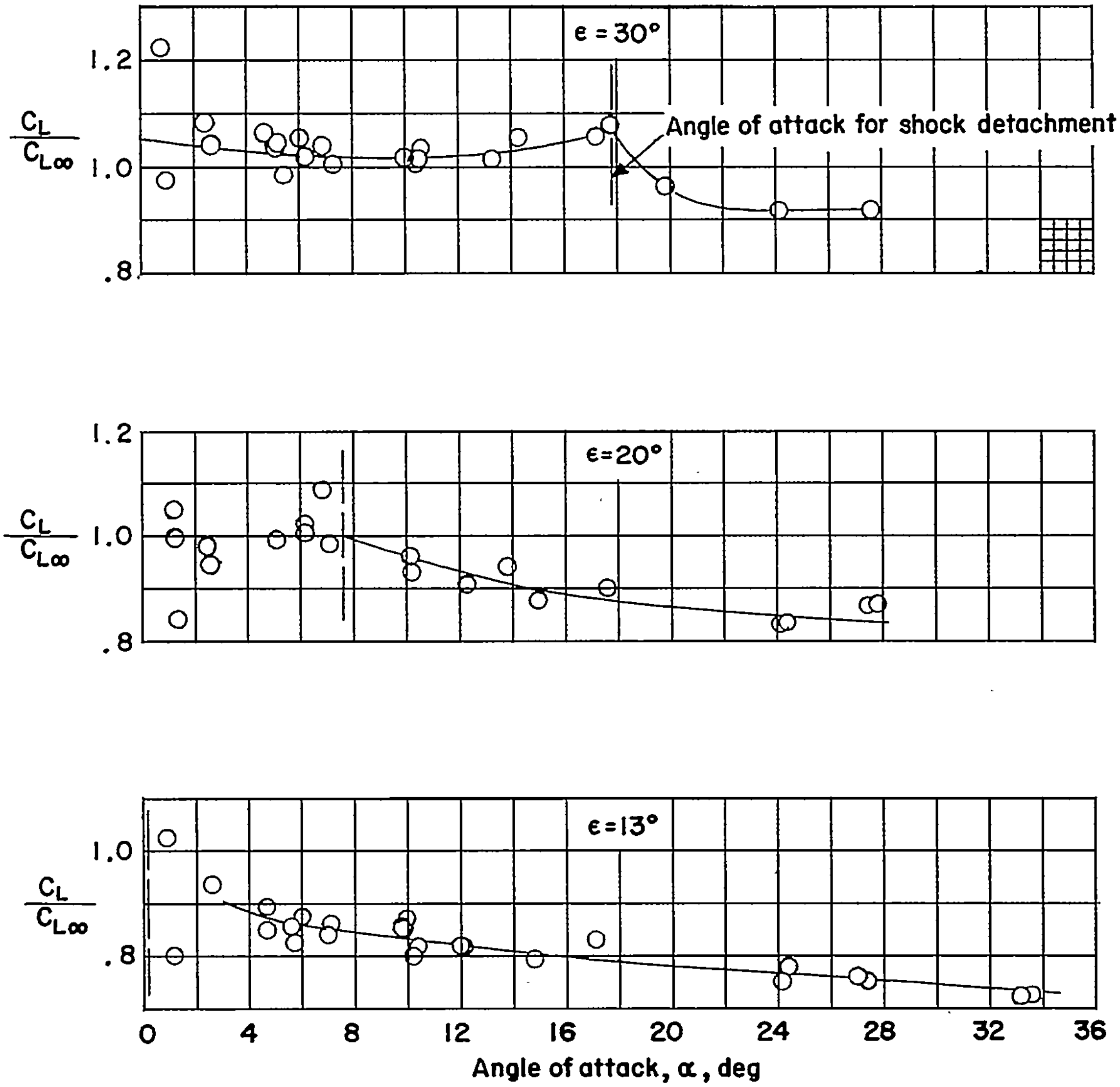

Figure 2.- The ratio of the lift coefficient of the 5-percent-thick delta wings to the two-dimensional shock-expansion lift coefficient as a function of angle of attack. M = 6.9.

[redacted]

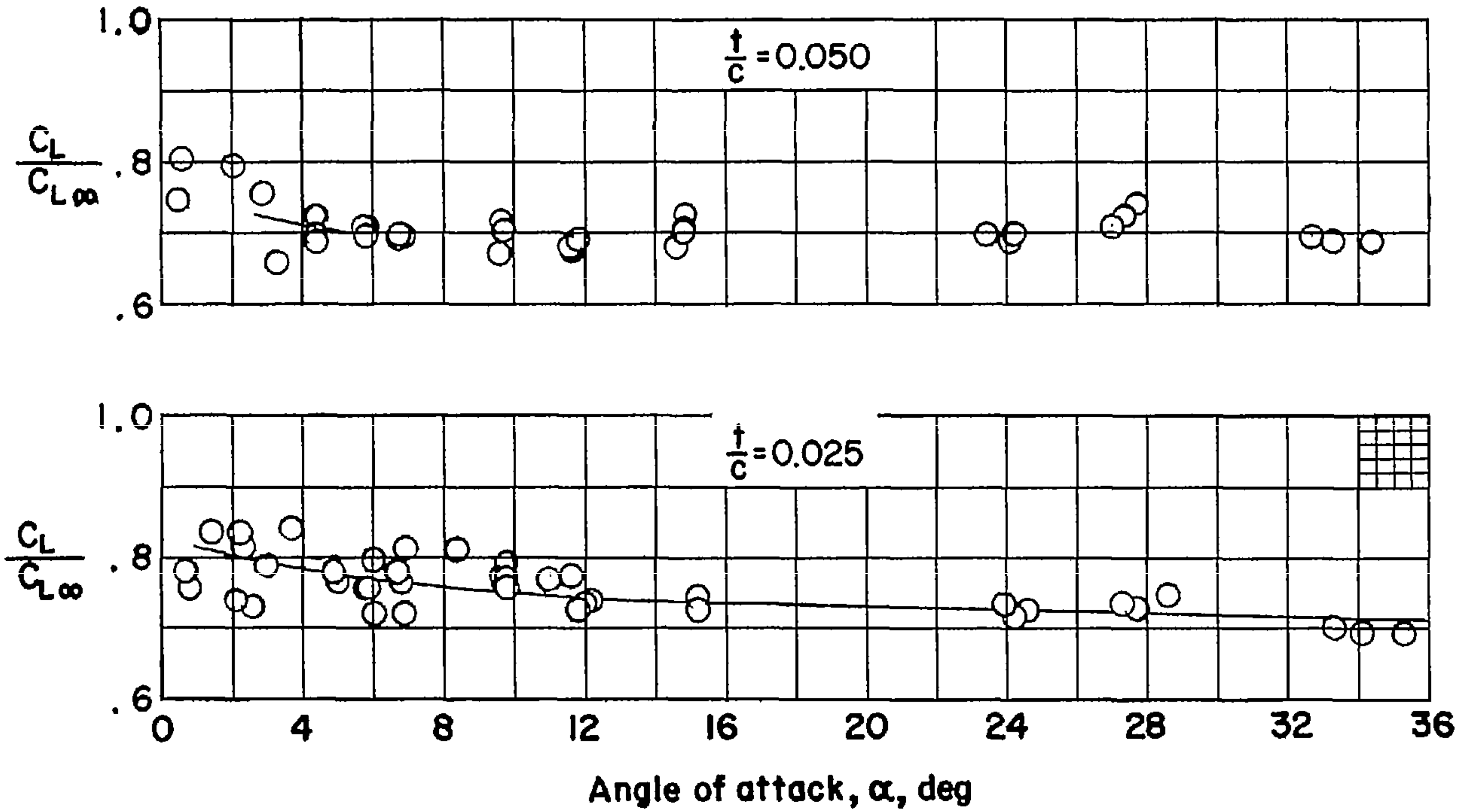

Figure 3.- The ratio of the lift coefficient of the delta wings with $\epsilon = 8^\circ$ to the two-dimensional shock-expansion lift coefficient as a function of angle of attack. $M = 6.9$.

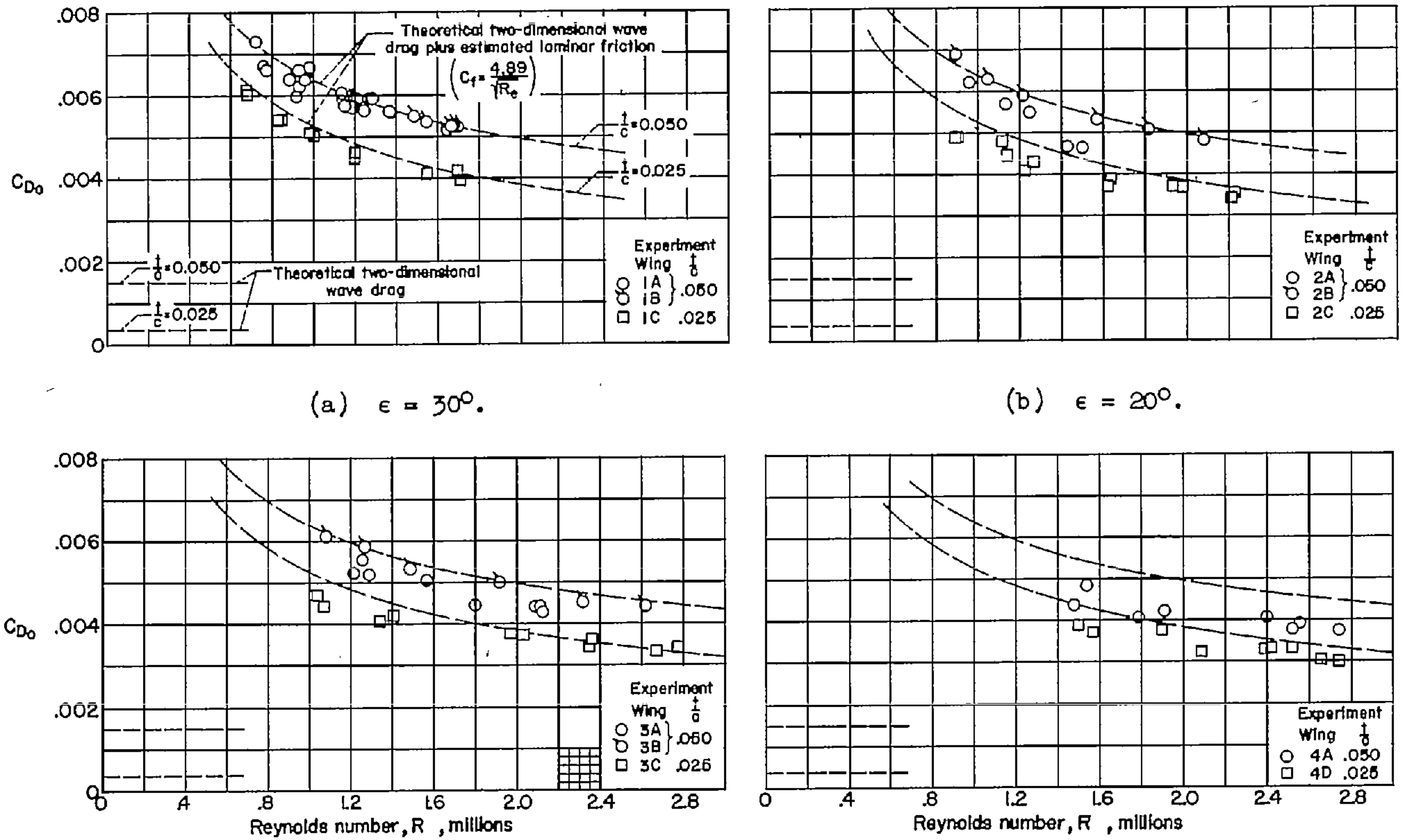

(a) ε = 30°.

(b) ε = 20°.

(c) ε = 13°.

(d) ε = 8°.

Figure 4.- The effect of Reynolds number on the drag coefficient at zero lift of the delta wings (Reynolds number based on root chord). M = 6.9.

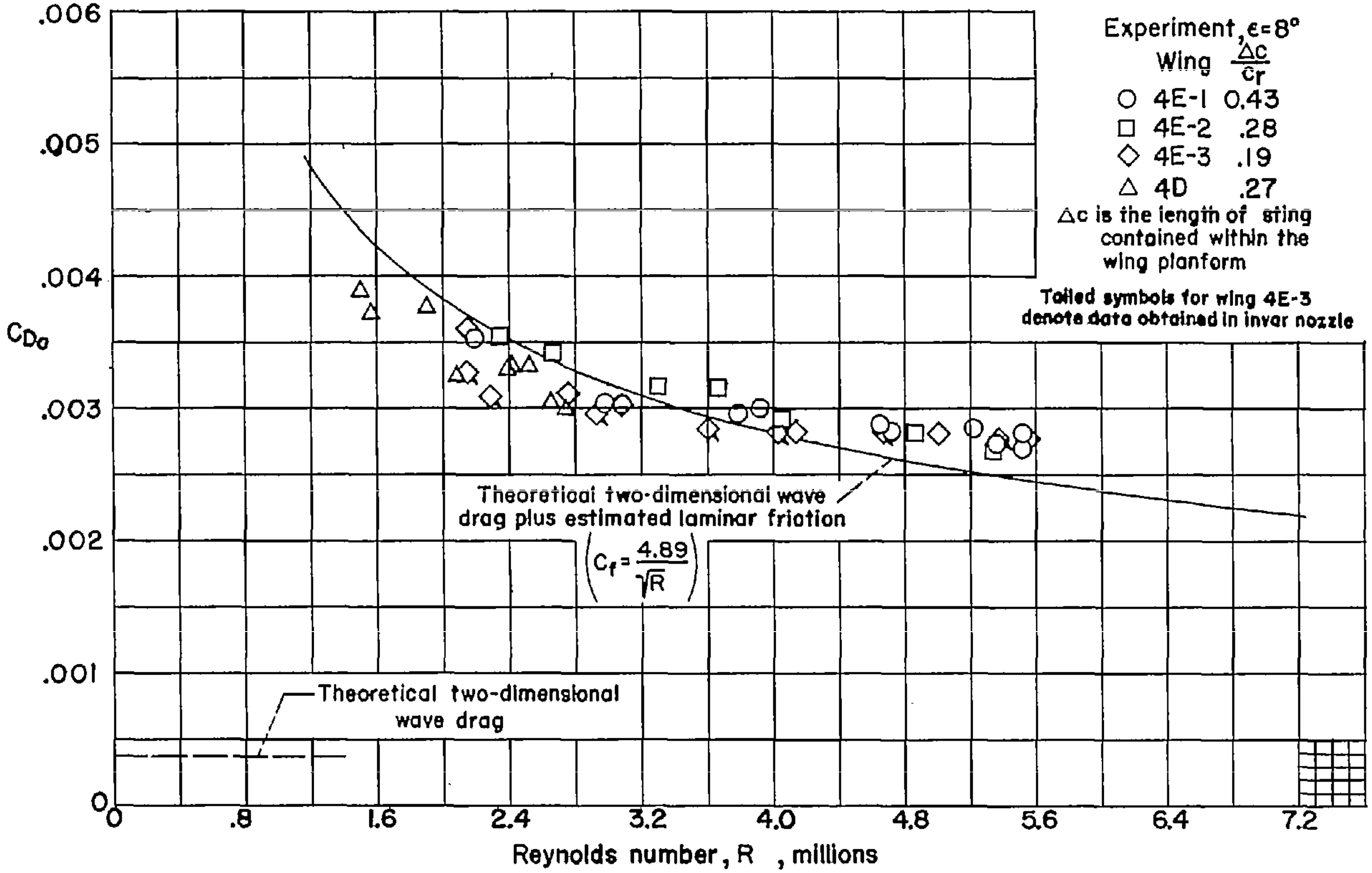

Figure 5.- The effect of Reynolds number on the drag coefficient at zero lift of the $2\frac{1}{2}$-percent-thick delta wing, $\epsilon = 8^{\circ}$. (Reynolds number based on root chord.) $M = 6.9$.

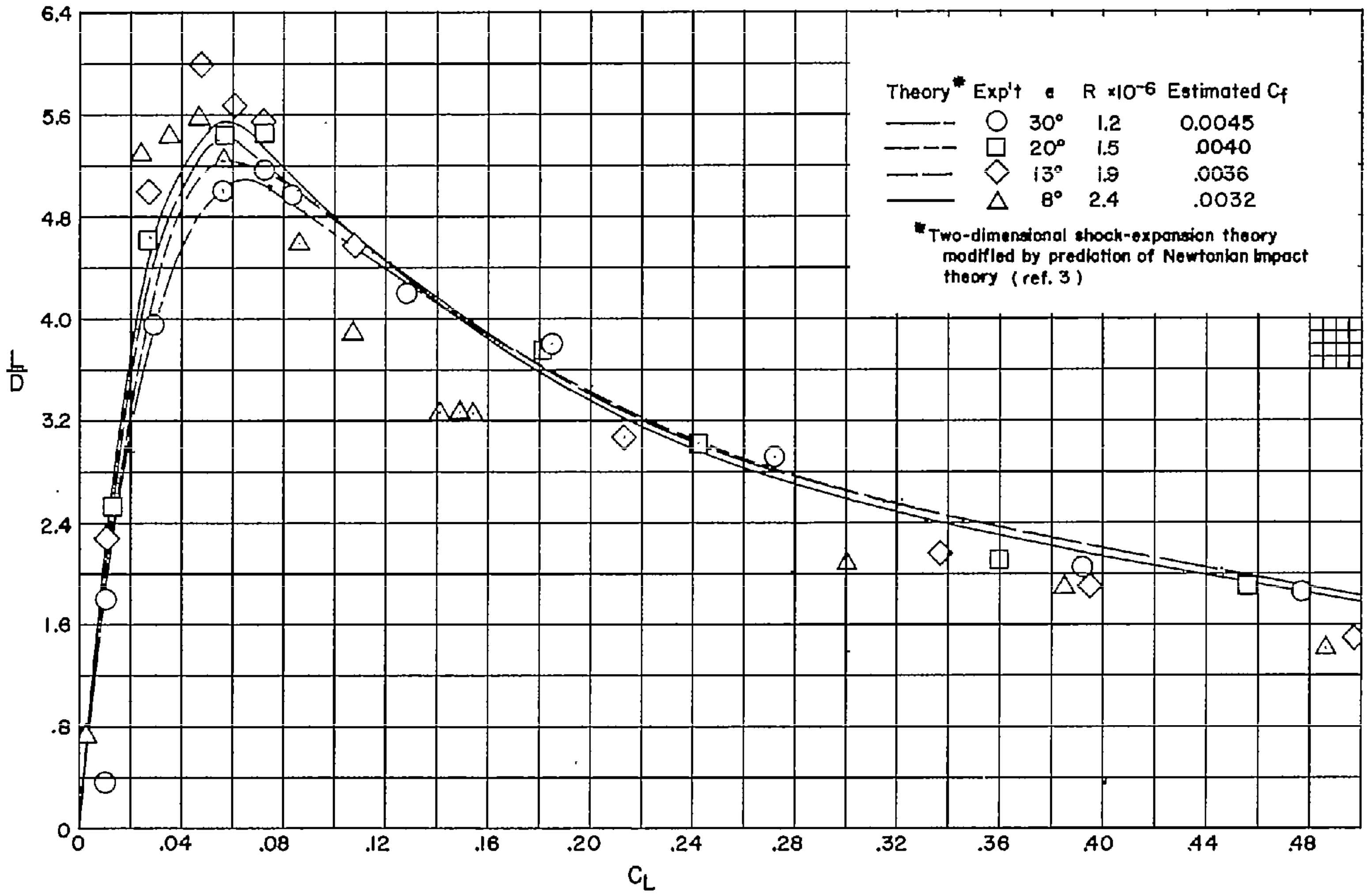

Figure 6.- The lift-drag ratio as a function of the lift coefficient for various semiapex angles where the plan-form area is constant. $t/c = 0.050$, $M = 6.9$.

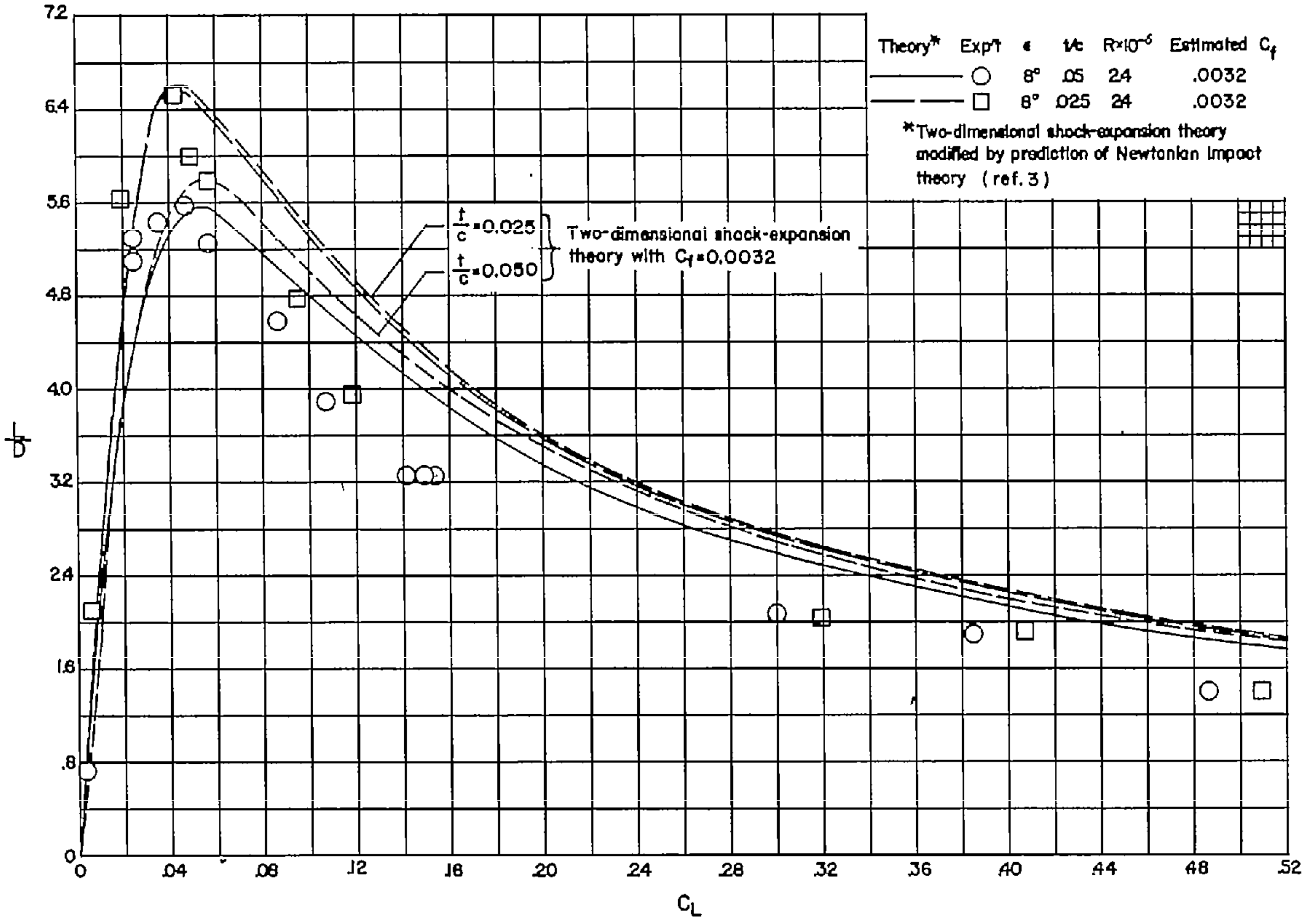

Figure 7.- The lift-drag ratio as a function of the lift coefficient for two thickness ratios where the plan-form area is maintained constant. $\epsilon = 8^{\circ}$; M = 6.9.

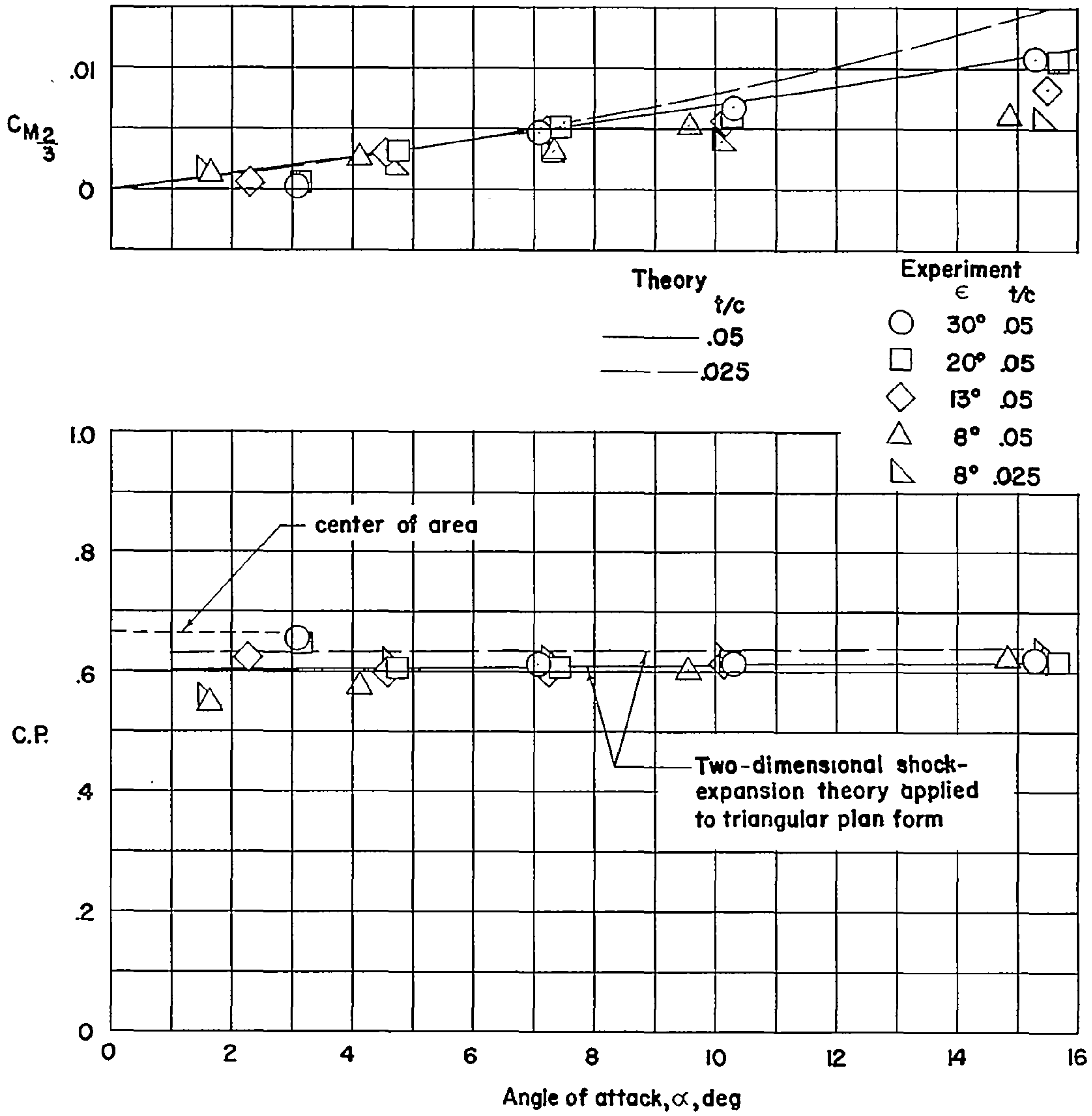

Figure 8.- The moment coefficient about the 2/3-root-chord point and center of pressure as a function of angle of attack. M = 6.9.

[redacted]

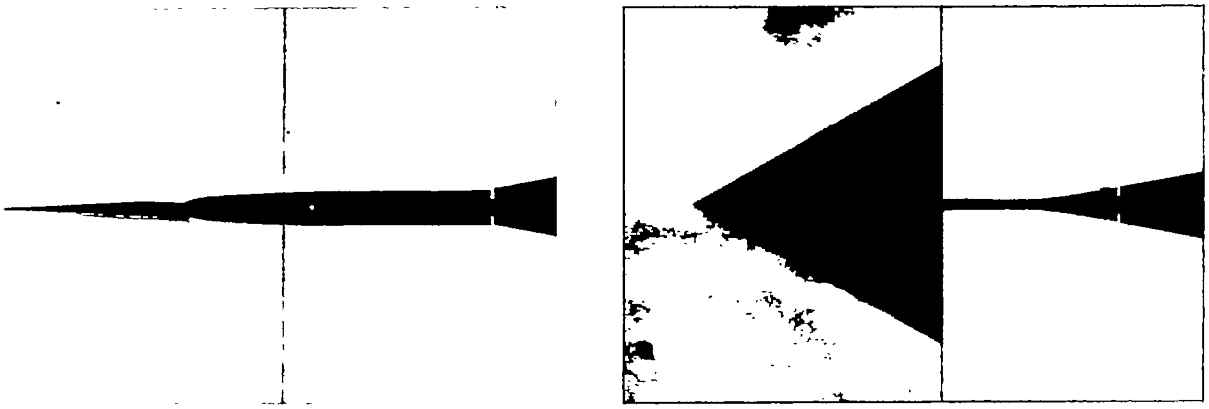

(a) $\alpha = 0^\circ$.

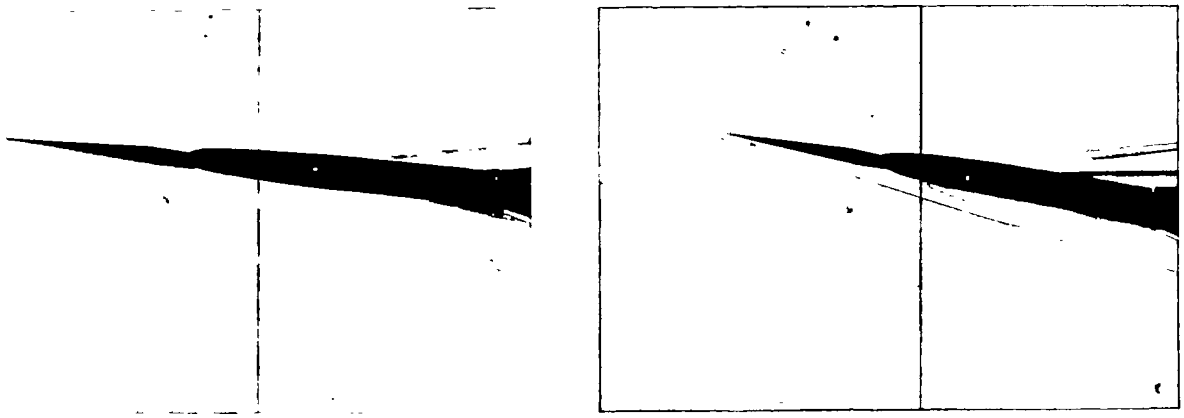

(b) $\alpha = 6.3^\circ$.

(c) $\alpha = 10^\circ$.

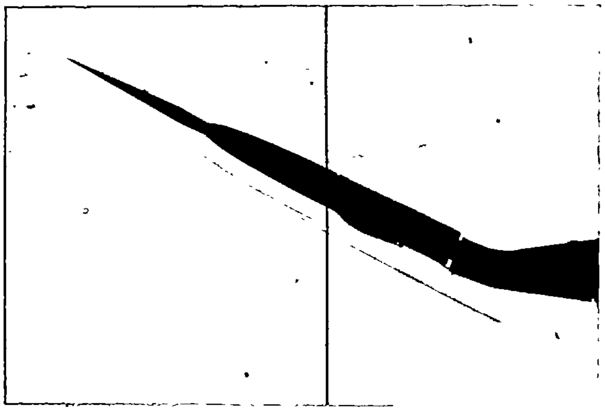

(d) $\alpha = 27.7^\circ$.

L-87892

Figure 9.- Schlieren photographs of wings 1A and 1B ($\epsilon = 30^\circ$, $t/c = 0.05$) at various angles of attack. $M = 6.9$.

[redacted]

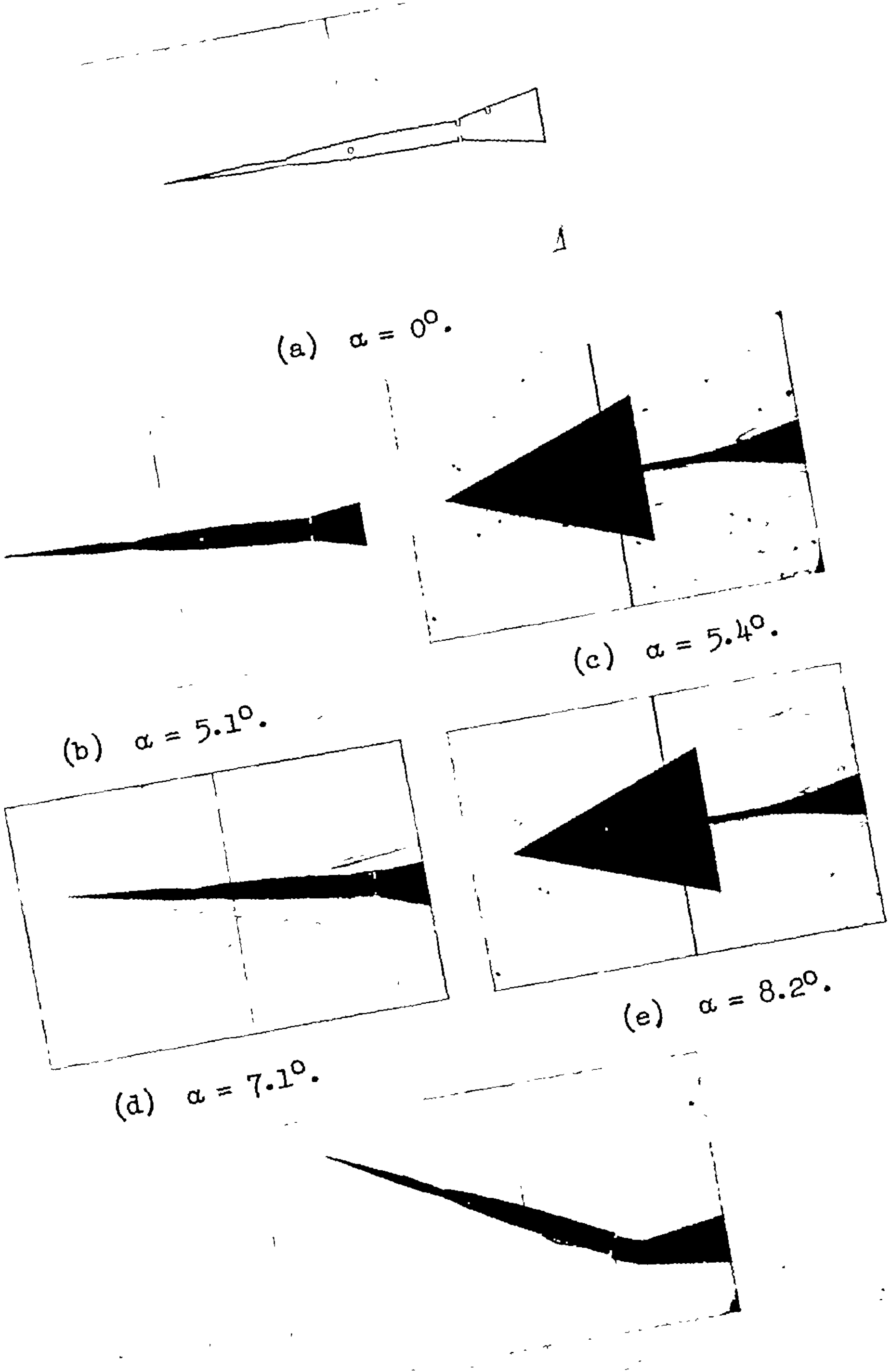

(a) $\alpha = 0^{\circ}$.

(b) $\alpha = 5.1^{\circ}$.

(c) $\alpha = 5.4^{\circ}$.

(d) $\alpha = 7.1^{\circ}$.

(e) $\alpha = 8.2^{\circ}$.

(f) $\alpha = 27.4^{\circ}$.

L-87893

Figure 10.- Schlieren photographs of wing 2A ($\epsilon = 20^{\circ}$, $t/c = 0.05$) at various angles of attack. $M = 6.9$.

[redacted]

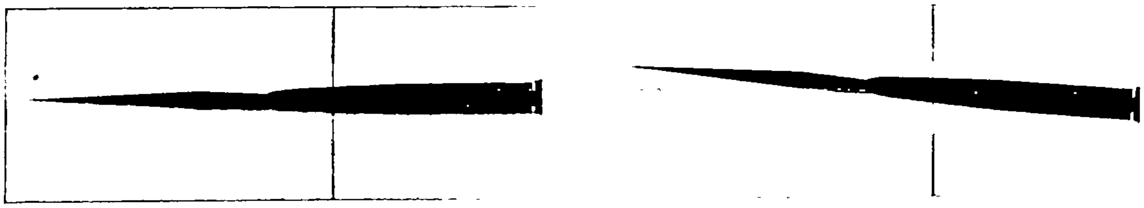

(a) $\alpha = 0^{\circ}$.

(b) $\alpha = 4.7^{\circ}$.

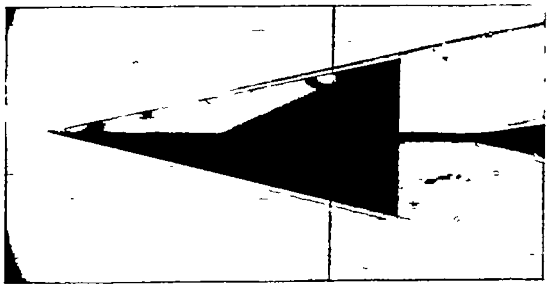

(c) $\alpha = 5.8^{\circ}$.

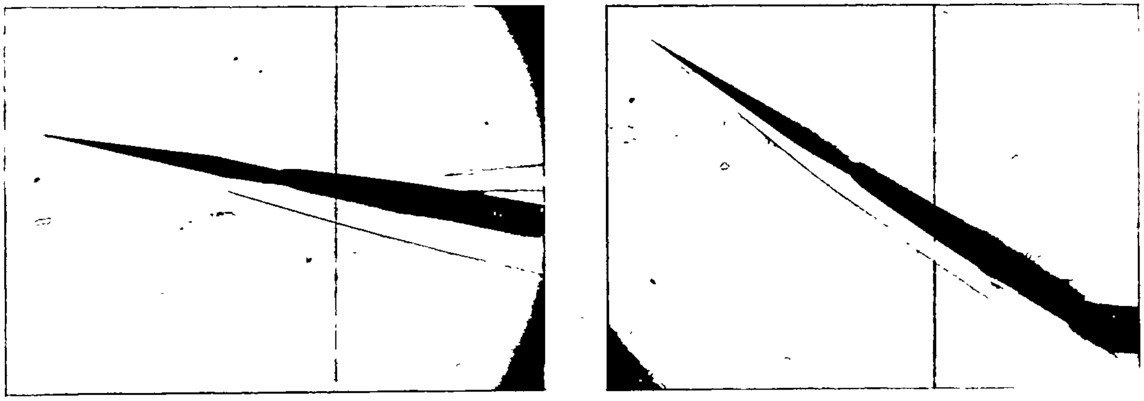

(d) $\alpha = 9.9^{\circ}$.

(e) $\alpha = 33.6^{\circ}$. L-87894

Figure 11.- Schlieren photographs of wing 3A ($\epsilon = 13^{\circ}$, $t/c = 0.05$) at various angles of attack. $M = 6.9$.

[redacted]

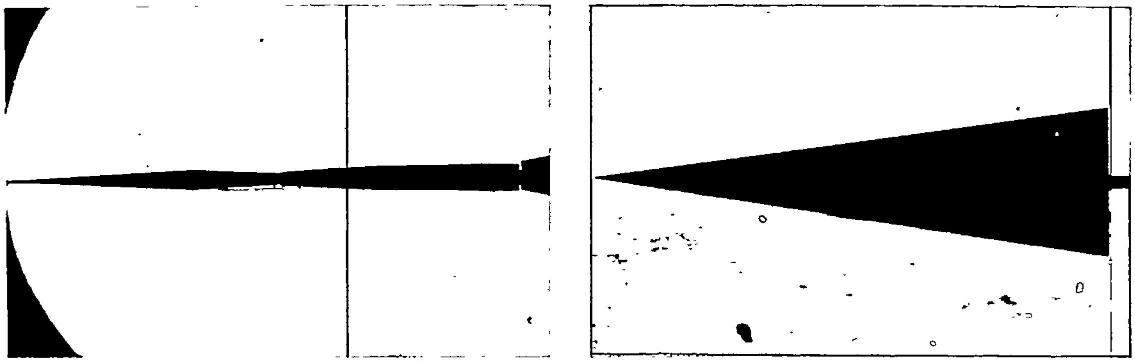

(a) $\alpha = 0^\circ$.

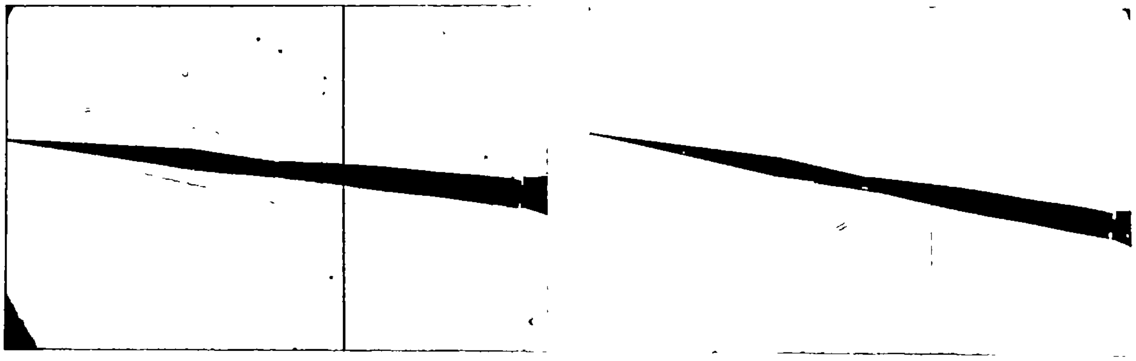

(b) $\alpha = 5.8^\circ$.

(c) $\alpha = 9.6^\circ$.

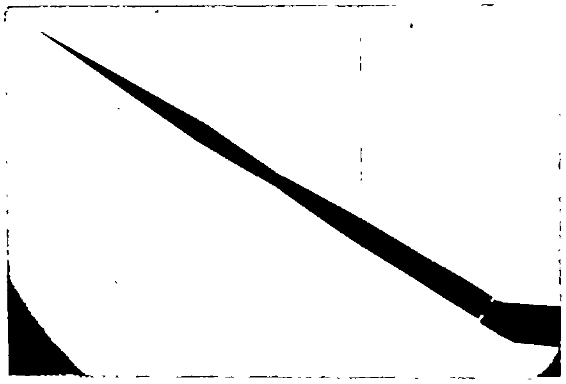

(d) $\alpha = 32.7^\circ$.

L-87895

Figure 12.- Schlieren photographs of wing 4A ($\epsilon = 8^\circ$, $t/c = 0.05$) at various angles of attack. $M = 6.9$.

[redacted]

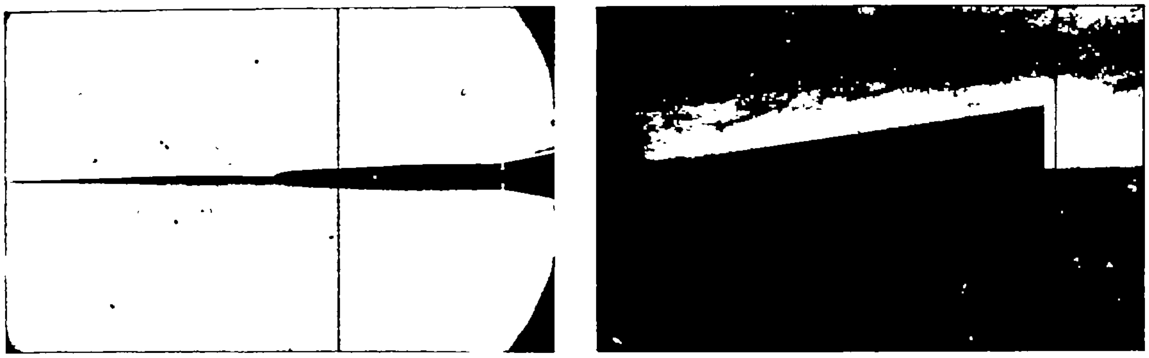

(a) α = 0°.

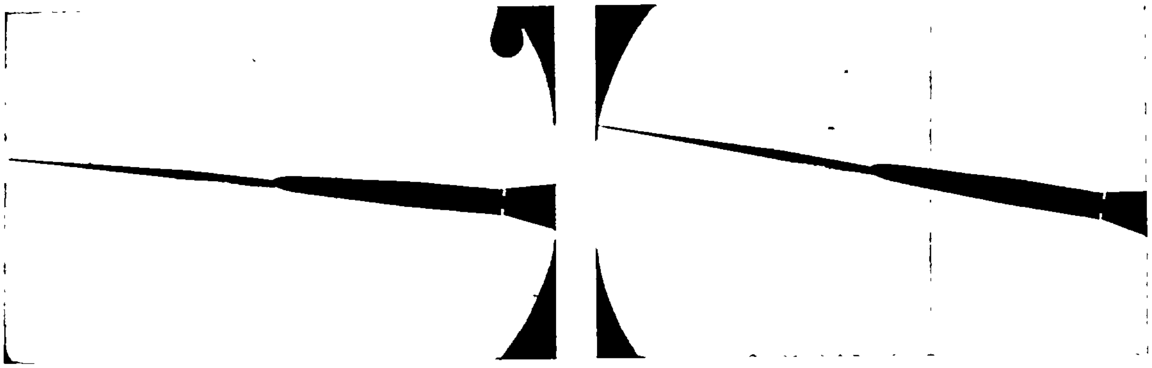

(b) α = 5.9°. (c) α = 9.8°.

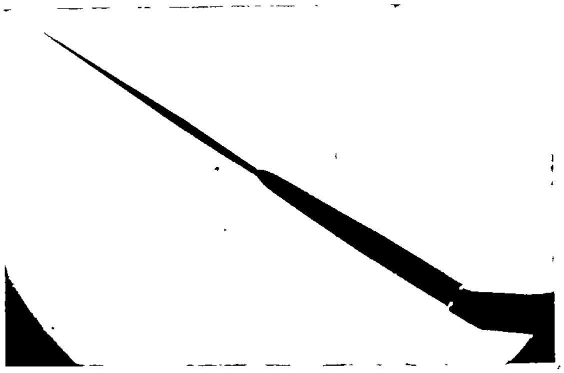

(d) α = 35.3°.

L-87896

Figure 13.- Schlieren photographs of wing 4D ($\epsilon = 8^\circ$, $t/c = 0.025$) at various angles of attack. $M = 6.9$.

[redacted]

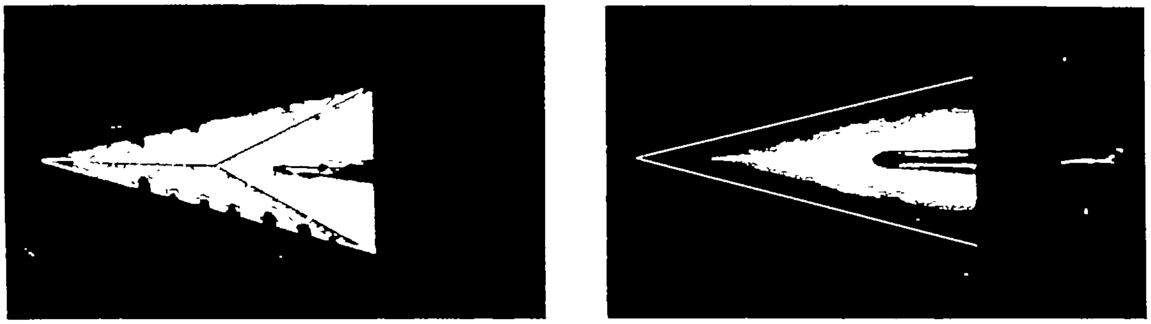

(a) No flow. (b) $\alpha = 0^{\circ}$.

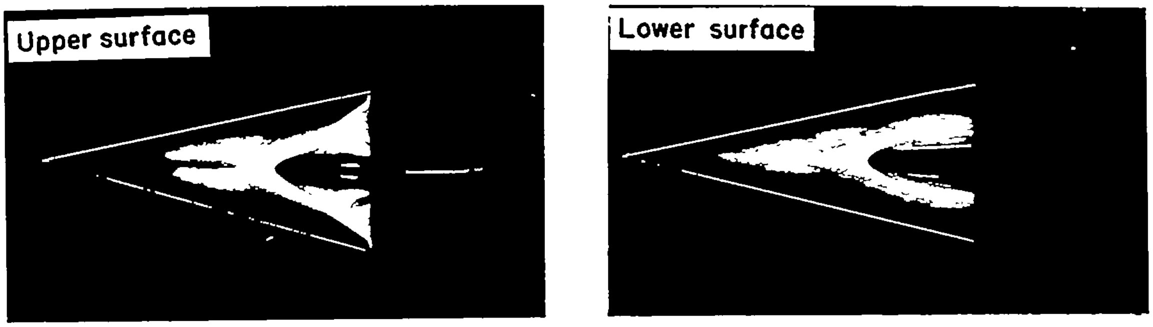
Upper surface
Lower surface

(c) $\alpha = 5.7^{\circ}$.

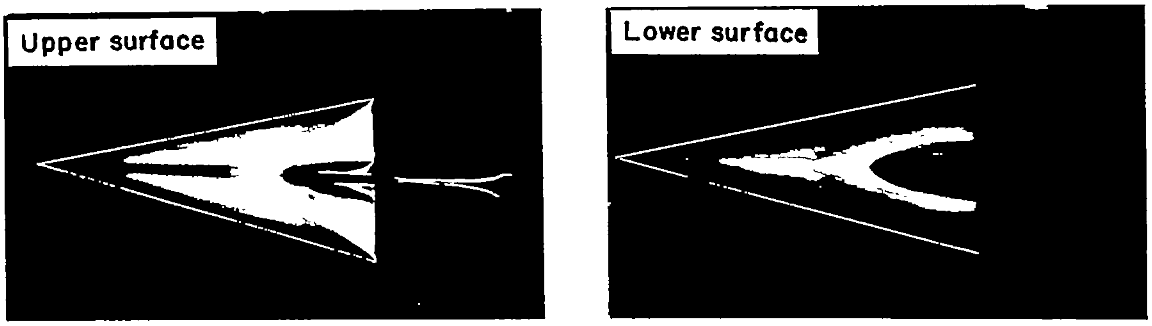
Upper surface
Lower surface

(d) $\alpha = 7.6^{\circ}$. L-87897

Figure 14.- Surface fluid flow studies of wing 3A ($\epsilon = 13^{\circ}$; $t/c = 0.05$) at various angles of attack. $M = 6.9$; $R = 2.1 \times 10^{6}$.

[redacted]

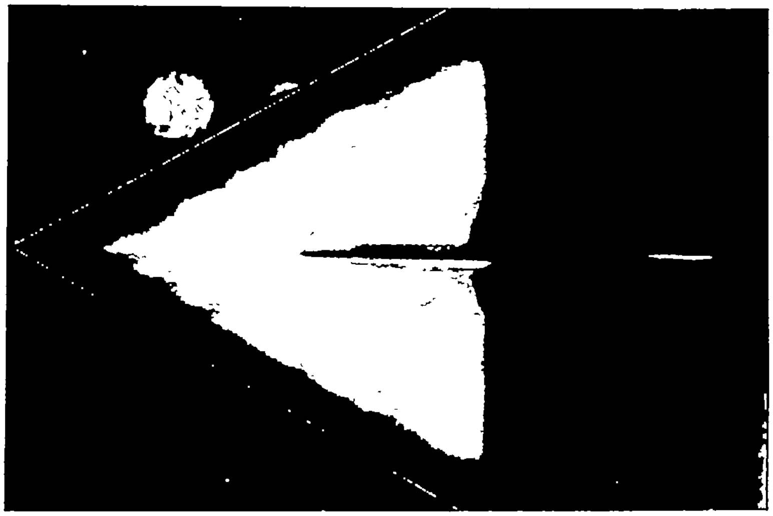

(a) Wing 1C; $\epsilon = 30^\circ$; $R = 1.7 \times 10^6$.

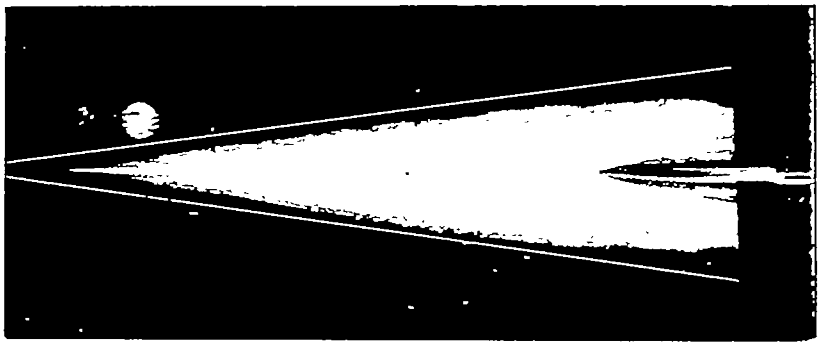

(b) Wing 4E-3; $\epsilon = 8^\circ$; $R = 5.3 \times 10^6$.

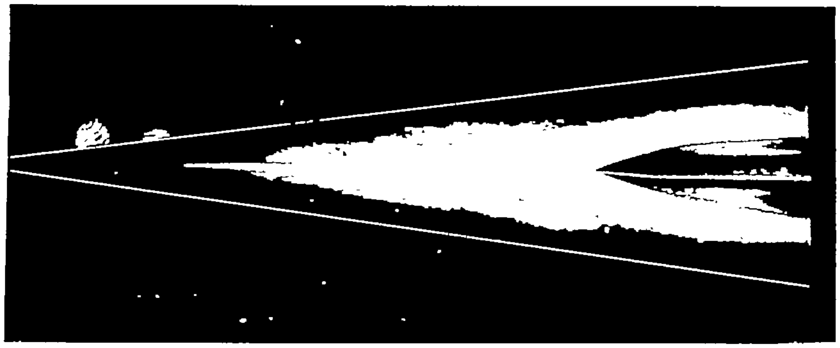

(c) Wing 4E-2; $\epsilon = 8^\circ$; $R = 3.4 \times 10^6$. L-87898

Figure 15.- Surface fluid flow studies of two of the $2\frac{1}{2}$-percent-thick delta wings at zero angles of attack. $M = 6.9$.

[redacted]

NACA-Langley - 4-14-55 - 350